RESEARCH MEMORANDUM

APPLICATION OF STATISTICAL THEORY TO BEAM-RIDER GUIDANCE IN THE PRESENCE OF NOISE. II - MODIFIED WIENER FILTER THEORY

By Elwood C. Stewart

Ames Aeronautical Laboratory
Moffett Field, Calif.

NATIONAL ADVISORY COMMITTEE
FOR AERONAUTICS

WASHINGTON
August 23, 1955

TABLE OF CONTENTS

	Page
SUMMARY	1
INTRODUCTION	1
SYMBOLS	2
GENERAL CONSIDERATIONS	3
ANALYSIS, RESULTS, AND DISCUSSION	6
The Modified Wiener Theory	6
Application of Modified Wiener Theory to the Beam-Rider Guidance System	8
Simplifications	9
General solution with control motion restriction	10
Effects of control-deflection restriction	12
Characteristics of the optimum transfer functions	13
Effect of noise magnitude on performance	14
System synthesis	15
Comparisons and other considerations	16
CONCLUDING REMARKS	17
APPENDIX A - DETERMINATION OF THE OPTIMUM MODIFIED WIENER FILTER	19
APPENDIX B - MISSILE-CONTROL-SYSTEM APPROXIMATION TO THE OPTIMUM TRANSFER FUNCTION	31
REFERENCES	34
TABLES	35
FIGURES	37

NATIONAL ADVISORY COMMITTEE FOR AERONAUTICS

RESEARCH MEMORANDUM

APPLICATION OF STATISTICAL THEORY TO BEAM-RIDER GUIDANCE IN THE PRESENCE OF NOISE. II - MODIFIED WIENER FILTER THEORY

By Elwood C. Stewart

SUMMARY

A study has been made of the application of Newton's modification of the Wiener filter theory to the optimization of a beam-rider guidance system operating in the presence of glint noise. Target and missile motions are assumed to be coplanar.

The theory has been applied using a typical variable-incidence missile by placing a realistic restriction on the mean-square surface deflection so that the system operation is confined to the linear range. The transfer functions of the optimum guidance system are derived and an example missile-control system is synthesized. It is shown that the minimum attainable error corresponding to a realistic control restriction is close to that for the Wiener theory. Performance of the system versus noise magnitude is given.

It is shown that the most critical saturable quantity is control deflection since constraining control deflections to realistic values can prevent saturation of other important quantities. Servo energy requirements are also greatly reduced in comparison with systems in which saturation is allowed to occur.

INTRODUCTION

Noise effects in missile-guidance systems impose one of the most serious limitations on the effectiveness of a missile. Noise signals in general have the effect of adding to the system false information which cannot be distinguished from true information. Thus the missile responds to the noise signals as well as to the true signal; the miss distance is thereby increased. Since many sources of noise (such as angular scintillation) are inherent in the physical mode of operation and cannot be

removed, it is important that missile systems be designed to minimize the miss even though the noise is present. Statistical filter theory is useful in performing this minimization.

One of the most valuable theories has been developed by Wiener (refs. 1 and 2). A previous report has considered the application of this theory to the minimization of the effects of radar glint noise in a beam-rider guidance system (ref. 3). It was found there that the optimum performance specified by the theory could not be obtained because of certain practical restrictions, as for example limiting of control deflection. Further study showed, however, that even in the presence of limiting, the optimum performance could be approached by the addition of network filtering to the guidance system. On the other hand, the optimum form for the added filtering could not be determined from this study since the system design was based on a theory which did not take into account the finite range of operation of the saturable quantities. In the present report an attempt is made to overcome this deficiency by determining the optimum transfer function under this last restriction. The theory for such an approach was made available in a paper by G. C. Newton (ref. 4) on a modification of the Wiener theory.

In the application of this theory to the missile guidance problem it is necessary to make certain assumptions. The main assumption made in reference 3, that is, the assumption that the target and missile move in the same plane, also will be made here. Other assumptions, such as those relating to the class of target maneuvers and noise, are discussed in the text.

SYMBOLS

H_{co}	transfer function of optimum compensating network
H_f	transfer function of the fixed network
N	noise magnitude or zero frequency spectral density, ft^2/radian/sec
T_N	time constant of the noise spectrum shaping filter, sec
Y_o	optimum closed-loop transfer function
a	acceleration of target maneuver, ft/sec^2
k	twice the average switching rate of target acceleration, 1/sec
y_T	target displacement from a space reference, ft
y_N	apparent target displacement from true target center due to noise, ft

y_M missile displacement from a space reference, ft

Φ_{id} cross-spectral density of the input signal with the desired output

Φ_{ii} spectral density of the input signal

Φ_N spectral density of noise displacement y_N, ft^2/radian/sec

Φ_T spectral density of target displacement y_T, ft^2/radian/sec

ϵ error between target and missile position, $y_T - y_M$, ft

ϵ_T component of error ϵ due to target motion, ft

ϵ_N component of error ϵ due to noise, ft

ρ Lagrangian multiplier

δ control-surface deflection, radians

ψ angle of yaw, radians

μ_o optimum open-loop transfer function

μ open-loop transfer function of system approximation to μ_o

ω angular frequency, radians/sec

$\overline{(\ )}$ complex conjugate of ( )

GENERAL CONSIDERATIONS

Glint noise is a term that is used to describe a shift in the apparent target location as determined by a radar. It is due basically to the variable reflection characteristics of aircraft targets and arises from the relative movement of the various reflecting surfaces. Since the radar utilizes the reflected signal to determine target location, variations in the reflected signal are interpreted by the radar as shifts in the target location. Of the many sources of noise which may exist in a missile-control system, glint noise is one of the most serious since it has a physical origin which cannot be eliminated, imposing a fundamental limitation on missile effectiveness. The situation in regard to glint noise is illustrated in figure 1(a) where the true target position is indicated as y_T and the glint noise is represented by the displacement y_N.

The present report is restricted to a two-dimensional study in which the target and missile move in a horizontal plane.[1] The guidance system is considered to be of the beam-rider type illustrated in figures 1(a) and 1(b). It should be noted here that displacements are referred to a fixed space reference. The general problem of the guidance system is to make the missile position coincide as closely as possible with the true target position y_T. The difference $y_T - y_M$ is indicated on this figure by the error ϵ, which obviously should be minimized. The criterion of merit which will be used here is the conventional mean-square time average of the error. This criterion is particularly appropriate in the case of the beam-rider system because the target-to-missile range is not normally transmitted to the missile; since the missile never knows when the target will be reached, it is reasonable to minimize the error for all values of time.

The design of a system normally depends on the inputs to be encountered, in this case the target motion and the noise. Because of their random nature neither of these quantities can be conveniently described explicitly as functions of time, and statistical descriptions are more suitable. In the following paragraphs the target motion and noise are briefly described.

The glint noise can be defined by specifying both the power spectrum or power spectral density as a function of frequency, and the amplitude distribution. Many measurements have been made on the characteristics of glint noise. (For a brief bibliography see ref. 3.) Although these measurements are somewhat complicated and uncertain, it is generally found that the amplitude distribution is approximately Gaussian and that the spectral density can be adequately represented by

$$\Phi_N = \frac{N}{T_N^2\omega^2 + 1} \tag{1}$$

An examination of glint noise spectra indicates that the break point $(1/2\pi T_N)$ is generally on the order of several cycles per second and as in reference 3 will be taken to be 6 cps, corresponding to $T_N = 0.0265$ second. The magnitude of the spectrum, N, of equation (1) depends on factors such as target size and target aspect so that the guidance system is generally forced to operate over a wide range of magnitudes. This range may extend from 7 ft^2/radian/sec for small targets up to around 30 ft^2/radian/sec for large bombers. For this range of magnitudes it might be thought that it would be necessary to optimize the system for each noise magnitude. As shown in reference 3, however, this was not the case for the method used therein since near-optimum results were obtained by optimizing only for a mid-range value called the design value. It is

[1]The complete three-dimensional problem would require a more complex analysis than used herein. Possibly either the present theory or Wiener's theory for multiple time series (ref. 1) could be applied to this case.

not unreasonable to believe that the same will hold for the method of the present report. As in reference 3, a design value of 15 ft^2/radian/sec will be used here.

Consider now the target maneuver. It is difficult to say exactly how a target will maneuver when under attack. A reasonable situation might be one in which the target maneuvers in some random manner to avoid being hit. As in reference 3, it is assumed that the target maneuvers laterally with maximum acceleration alternately in opposite directions. The duration of each acceleration is a random function determined by some distribution. A reasonable distribution which leads to an easily handled spectral density is the Poisson distribution $[(1/\bar{T})\exp(-T/\bar{T})]$, where T represents the time and $\bar{T}$ the average time between switches of the acceleration. The spectral density of the target acceleration for this maneuver is described by

$$\Phi_{\ddot{y}_T} = \frac{ka^2}{\pi(\omega^2 + k^2)}$$

Here the quantity a represents the magnitude of the target acceleration normal to the beam, and k is twice the average switching rate or $k = 2/\bar{T}$. The spectral density of the target displacement is then given by

$$\Phi_T \equiv \Phi_{y_T} = \frac{ka^2}{\pi\omega^4(\omega^2 + k^2)} \tag{2}$$

Because of the ω^4 in the denominator it would appear that there is a problem here concerning the existence of this spectral density. However, it can be shown that it is possible to use this representation for purposes of computations (see Appendix A). For the typical tail-chase maneuver to be used in a later example the target is assumed to maneuver with ± 1 g acceleration at an average period of 5 seconds, which gives $a = 32.2$ ft/sec^2 and $k = 0.4$ switch/sec.

It should be pointed out that an optimum design based on the above target maneuver will operate efficiently against this class of maneuver as a whole, although not necessarily efficiently against one particular target maneuver such as a single target turn. However, as indicated in reference 3, this design will be essentially optimum for the single-turn maneuver as well.

ANALYSIS, RESULTS, AND DISCUSSION

The Modified Wiener Theory

The primary objective of the modified Wiener theory is to arrive at an optimum transfer function in which the effects of certain saturating elements are considered. Ideally it would be desirable to determine this optimum transfer function without any assumptions about whether or not the system would operate in these saturation regions. However, no such theory is available at present. The approach considered herein is one in which the transfer functions of certain available elements are chosen so that saturation does not occur. Thus the system is forced to remain linear and linear methods are immediately applicable. Although it is not apparent at first glance, there are certain indications that this approach may lead to desirable results. First, it appears intuitively that saturation is undesirable because of the loss of both intelligence and ability to control the missile when in the saturated regions. Second, it is indicated in reference 3 that the undesirable effects of saturation can be reduced by the addition of filtering without undue increase in the error; this method in effect tends to keep the operation of the system in the linear range. These are only indications, however, and the real justification in the completely linear approach depends on the resultant error performance which can only be established by investigation.

The theory to be used in this approach follows Newton's modification of the Wiener filter theory. To describe the essentials of the theory it will be convenient to refer to figure 2 where the block diagram corresponding to the general filter problem is given. It should be noted that the notation here corresponds to that in reference 4. In the general situation there are usually certain elements that are given and may not be altered in the design of the system. These elements are denoted by the transfer function H_f in the figure. In particular cases the fixed elements might represent missile aerodynamics, servo motors, and so forth, depending on the application. To describe the limiting or saturating quantities it is necessary to express them in terms of the fixed elements and either the input or output of the system. Which choice is made depends on the location of the fixed elements - if the output element is fixed, as is usually the case, it is desirable to express the saturating quantities in terms of the output. Figure 2 illustrates a situation wherein the output element is fixed. At this point it is necessary to know the saturating quantities. For this purpose we introduce a fictitious situation. Since in the general case the saturating quantities are different from the input to the fixed network, the input to H_f in figure 2 is imagined to be fed through certain transfer functions H_{sn} which act as recording elements and whose outputs are the saturating quantities θ_{sn}. It should be pointed out that according to this formulation of the problem the outputs of the saturating elements do not feed into the system but are used merely for the purpose of evaluation. From

the above discussion, then, it is clear that by specifying both the fixed and saturating networks, the saturating quantities can be related to the output. The remainder of the system, indicated in figure 2 by the compensating network H_{co} is unknown and must be determined according to a specified criterion of merit.

By way of comparison, the original Wiener theory considers only the problem of choosing the over-all transfer function so as to result in minimum mean-square error, θ_ϵ, between the actual output, θ_o, and the desired output, θ_d. The modified theory, however, considers the minimization of this same mean-square error with a side restriction on the available range of operation of the limiting quantities; for mathematical reasons it is convenient to consider this restriction to be in the form of a mean-square limitation. According to the method of Lagrange (ref. 5) this means that the quantity to be minimized is of the form

$$\theta_\epsilon + \sum_{n=1}^{N} \rho_n \theta_{sn} \tag{3}$$

where the ρ_n's represent Lagrangian multipliers which must be chosen properly to restrict the operation of the saturable quantities θ_{sn} to very nearly the linear range.

In most cases it is possible to control saturation by an appropriate choice of the mean-square value of the saturating quantities θ_{sn}. In the simple case when a quantity has a Gaussian distribution of amplitudes the relation between the mean-square value of this quantity and the probability of its limiting is well known and particularly simple. The distribution of the saturating quantity in the actual case may not be Gaussian for either of two reasons: First the input may not be Gaussian or, second, there may be several saturating quantities which interact. On the other hand, even in these cases the distribution is frequently near enough to Gaussian that saturation can be readily controlled by an appropriate choice of mean-square value.

The derivation of the solution for the optimum compensating network which minimizes the expression (3) is beyond the scope of this report, but as shown in reference 4 an expression for this network is

$$\left.\begin{aligned} H_{co}(i\omega) &= \frac{1}{2\pi\Lambda^+(\omega)} \int_0^\infty e^{-i\omega t} \int_{-\infty}^{\infty} \frac{\overline{H_f(i\alpha)}\Phi_{id}(\alpha)e^{i\alpha t}}{\Lambda^-(\alpha)}\, d\alpha\, dt \\ \text{where} \\ \Lambda(\omega) &= \left[\overline{H_f(i\omega)}H_f(i\omega) + \sum_{n=1}^{N} \rho_n \overline{H_{sn}(i\omega)}H_{sn}(i\omega)\right]\Phi_{ii}(\omega) \end{aligned}\right\} \tag{4}$$

In this equation the Φ quantities represent certain combinations of target motion and noise spectral densities (see Appendix A), H_f refers to the fixed network transfer function, H_{sn} refers to the transfer function of the nth saturating component, and ρ_n represents the corresponding Lagrangian multiplier. Of these quantities, all will normally be known with the exception of the ρ_n. This means that only the form of H_{co} is known from this equation since the numerical constants depend on the values of ρ_n. The ρ_n, however, are implicitly related (ref. 4) to the mean-square restrictions on θ_{sn} by the following equation

$$\overline{\theta_{sn}^2} = \int_{-\infty}^{\infty} \overline{H_{co}(i\omega)} H_{co}(i\omega) \overline{H_{sn}(i\omega)} H_{sn}(i\omega) \Phi_{ii}(\omega) d\omega \qquad (5)$$

Here it is to be noted that the integrand in equation (5) is dependent on the $\rho_1, \rho_2, \ldots, \rho_N$ by virtue of the dependence of H_{co} on these quantities (eq. (4)). It can be shown that in many cases of interest the ρ_n's are uniquely determined by the equations (4) and (5) when a suitable mean-square value, $\overline{\theta_{sn}^2}$, is chosen. This quantity is to be chosen so as to limit the probability of saturation to a small value according to a criterion given later. In most practical applications the complexity of the operations involved in solving these equations does not permit the general solution to be obtained explicitly in terms of the input characteristics and fixed networks. In spite of this a great deal can be learned from certain numerical solutions, as will be shown.

Application of Modified Wiener Theory to the Beam-Rider Guidance System

The validity of the application of the modified Wiener theory to the beam-rider guidance problem depends on whether or not several restrictions inherent in the theory are met. In general, they are no stricter than are those of the unmodified Wiener theory. First, the input quantities, target motion and noise, must be stationary random series (see ref. 6 for a detailed definition) and defined by corresponding power spectra which are continuous. It is generally believed that displacements at the target are approximately stationary random series (ref. 3). Since the beam-rider system operates from these displacements, the inputs to the beam-rider system are also stationary random series. Second, the transfer function of the system must have constant coefficients. In general, however, the kinematic loop of guidance systems involves a time-variable range factor. In particular, for the beam-rider system the time-variable factor is the ratio of the launcher-to-missile and the launcher-to-target ranges. On the other hand, because the miss is determined primarily by what happens

near the end of flight during which the variation in this ratio is small, it is reasonable to assume that the requirement of constant coefficients is approximately met. Third, the transfer functions of the fixed and saturating components must be known.

Simplifications.- There are many quantities which may saturate in the beam-rider system; the most important are (1) control motion, (2) rate of control motion, and (3) radar receiver voltages. To apply the theory to all these nonlinearities simultaneously would be a tremendous task. However, there are indications that only one limiting quantity need be considered in the present problem.

One indication is that of the three types of limiting not all are of equal severity so that one type tends to predominate. Intuitively, it might be felt that control-motion limiting is the most serious type and that placing a restriction on the control motion will satisfactorily reduce the other types of limiting. Of course the validity of this presumption would require verification.

Another indication is that of the three types of limiting one is more fundamental in that it is more difficult to remove than the others. It will be noted that items (2) and (3) above are both control-system limitations while (1) is essentially an aerodynamic or mechanical limitation. Since control systems are relatively versatile and can be designed to cover a wide range of characteristics, it appears that control-motion limiting is the most fundamental to the problem.

From these indications it appears reasonable to consider only control-motion limiting. The validity of the assumption that reducing this one type of limiting will reduce the other types sufficiently will then be verified. In terms of figure 2 this simplification means that only one saturating-component transfer function, H_S, is involved. If the fixed network is chosen to be the aerodynamic transfer function so that the control motion is the input to the fixed network, then H_S equals unity. Thus, a block diagram more suited to the specific case of the beam-rider system would appear as in figure 3. It will be noted in figure 3 that the input quantity called θ_i in figure 2 has been split into the two parts which exist in the actual case, target motion y_T and noise y_N. Likewise the desired output θ_d of figure 2 is represented in figure 3 by the target motion y_T. The box H_{CO}, then, is that portion of the guidance system which is to be chosen to minimize the expression (3). It may be noted that in the form given the diagram does not bear a direct resemblance to the form of an actual guidance system since the latter will involve feedback loops. The form shown, however, typifies that of the general filter problem and is better suited to calculation. The solution of this problem can be readily converted to that of the actual beam-rider system.

A few additional remarks are appropriate concerning the two quantities Φ_{id} and Φ_{ii} in equation (4). If Φ_{ii} is defined as the autocorrelation function of the input in figure 2, then

$$\varphi_{ii}(\tau) = \lim_{T\to\infty} \frac{1}{2T} \int_{-T}^{T} \theta_i(t)\theta_i(t+\tau)dt$$

In terms of the input of figure 3, this becomes

$$\varphi_{ii}(\tau) = \lim_{T\to\infty} \frac{1}{2T} \int_{-T}^{T} [y_T(t) + y_N(t)][y_T(t+\tau) + y_N(t+\tau)]dt$$

$$\equiv \varphi_T(\tau) + \varphi_N(\tau) + \varphi_{TN}(\tau) + \varphi_{NT}(\tau)$$

It is normally assumed that there is no correlation between target motion and noise so that $\varphi_{TN}(\tau)$ and $\varphi_{NT}(\tau)$ are zero. It follows that the Fourier transform of $\varphi_{ii}(\tau)$ is

$$\Phi_{ii}(\omega) = \Phi_T(\omega) + \Phi_N(\omega)$$

Since in the present case the target motion and the desired output are identical it is easy to show in a similar fashion that

$$\Phi_{id}(\omega) = \Phi_T(\omega)$$

General solution with control motion restriction.- By virtue of the simplifications discussed in the previous paragraphs the application of the theory to a beam-rider-type guidance system becomes feasible. For the case illustrated by figure 3, the optimum compensating network, H_{co}, is given by

$$\left.\begin{aligned} H_{co}(i\omega) &= \frac{1}{2\pi\Lambda^+(\omega)} \int_0^\infty e^{-i\omega t} \int_{-\infty}^{\infty} \frac{\overline{H_f(i\alpha)}\Phi_T(\alpha)e^{i\alpha t}}{\Lambda^-(\alpha)}\, d\alpha\, dt \\ \text{where} \quad \Lambda(\omega) &= \left[\overline{H_f(i\omega)}H_f(i\omega) + \rho\right]\Phi_{ii}(\omega) \end{aligned}\right\} \quad (6)$$

In the above equation the quantities Φ_T and Φ_{ii} are known from the target motion and noise characteristics as previously discussed. The transfer function H_f of the missile aerodynamics was chosen for this study to represent that for a typical variable-incidence missile. The significant transfer functions for this missile are given by the following conventional equations (ref. 7)

$$\frac{\psi}{\delta} = \frac{1}{T_d} \frac{T_M s + 1}{s(T_a^2 s^2 + 2\zeta_a T_a s + 1)} \tag{7}$$

$$\frac{y_M}{\psi} = \frac{T_d}{T_s^2} \frac{T_b^2 s^2 + 2\zeta_b T_b s + 1}{s(T_M s + 1)} \tag{8}$$

from which the fixed network becomes

$$H_f = \frac{y_M}{\delta} = \frac{1}{T_s^2} \frac{T_b^2 s^2 + 2\zeta_b T_b s + 1}{s^2(T_a^2 s^2 + 2\zeta_a T_a s + 1)} \tag{9}$$

Table I summarizes the parameters for this particular missile at a given flight condition. It should be pointed out for later comparison purposes that these aerodynamics correspond to those used in the previous noise study, reference 3. The remaining parameter ρ is not known so that equation (6) can only be used to give the general form of H_{co}. To illustrate this, the form of H_{co} is derived in Appendix A where it is shown that

$$H_{co}(s) = T_s^2 \frac{s^2(T_\alpha^2 s^2 + 2\zeta_\alpha T_\alpha s + 1)(T_a^2 s^2 + 2\zeta_a T_a s + 1)}{(T_\beta s + 1)(T_\gamma^2 s^2 + 2\zeta_\gamma T_\gamma s + 1)(T_u^2 s^2 + 2\zeta_u T_u s + 1)(T_v^2 s^2 + 2\zeta_v T_v s + 1)} \tag{10}$$

Many of the factors involved in this equation are functions of the unknown parameter ρ. The exceptions are (1) the aerodynamic factors, that is, the gain T_s^2 and the second quadratic in the numerator, and (2) the terms due to target motion and noise characteristics, that is, the first two denominator factors. The remainder of the terms can only be evaluated after the proper value of ρ has been established. This value can be determined from the restriction placed on the mean-square control motion. The analog of equation (5) in the present case is

$$\overline{\delta^2} = \int_{-\infty}^{\infty} \overline{H_{co}(i\omega)} H_{co}(i\omega)[\Phi_T(\omega) + \Phi_N(\omega)]d\omega \tag{11}$$

In theory, equations (10) and (11) can be solved for the compensating network, H_{co}, corresponding to an arbitrary mean-square control motion, $\overline{\delta^2}$. In this application, however, because of the complexity of the fixed network and the input quantities, the computation is unwieldy. Alternatively the following procedure will be used here: First calculate the function H_{co} from equation (10) for a selected value of ρ. After the result is inserted in equation (11), evaluation of the integral gives a value of $\overline{\delta^2}$. By repetition of this process for a few judiciously

selected values of ρ it is possible to determine the value of ρ corresponding to the desired mean-square restriction $\overline{\delta^2}$.

As mentioned previously, H_{co} does not exist, as such, in the beam-rider guidance system. The relationship between the filter problem being solved and the actual beam-rider system is illustrated by a comparison of figures 3 and 4. From figure 3 it is apparent that if the entire guidance-system transfer function is represented by Y_o, then

$$Y_o = H_{co}H_f \tag{12}$$

Thus the solution for the compensating network H_{co} determines the desired over-all transfer function Y_o for the actual form of beam-rider system shown in figure 4.

Unfortunately, the theory does not give the performance of this optimum system directly in terms of the resultant error. The minimum error can be found, however, from the following relationship (ref. 7)

$$\overline{\epsilon^2} = \overline{\epsilon_T^2} + \overline{\epsilon_N^2}$$

$$= \int_{-\infty}^{\infty} |1 - Y_o(i\omega)|^2 \Phi_T(\omega)d\omega + \int_{-\infty}^{\infty} |Y_o(i\omega)|^2 \Phi_N d\omega \tag{13}$$

Effects of control-deflection restriction.- The procedure discussed in the above paragraphs has been carried out for a range of values of the Lagrangian multiplier ρ. The results of this study are presented in figure 5 where the errors due to target motion and noise, the total error, and the control deflection are given as functions of ρ. These curves illustrate the nature of the restriction of the control deflection. Large values of ρ here correspond to a large restriction and therefore small control deflections. It is apparent from the expression (3) that as ρ decreases the restriction on control deflection is reduced until at $\rho = 0$ the Wiener case is reached. By cross-plotting these curves so as to eliminate the variable ρ which has no significance in itself, the curve of figure 6 is obtained. This curve is fundamental to the problem in that it illustrates the dependence of error on available surface deflection. Here the minimum obtainable error according to Wiener theory is indicated by the horizontal line off to the right. The curve is shown dotted in this region in order to indicate that these values of error would require unobtainable control deflections.

The importance of the curve of figure 6 is that it represents the theoretical lower limit of error corresponding to any restriction on root-mean-square control motion. Each point on the curve would be achieved by a different guidance-system transfer function. The interesting feature of this

curve is that as the surface deflection is reduced from large values, the minimum error increases relatively slowly over an appreciable range of obtainable control deflections. To determine the best operating point on the curve it is necessary to specify the degree to which limiting will be allowed to occur. Since in this linear case the control deflection is Gaussian, an rms control deflection of half the maximum allowable deflection would then restrict it to within these limits about 95 percent of the time (ref. 8). For the specific missile being used in this study the maximum control deflection is about 15° which would put the desired operating point at 7.5° as indicated in figure 6. It can be seen from figure 6 that for this operating point the effect of this restriction is an increase in error of about six feet above that of the Wiener theory. It is a somewhat surprising result that the increase in error is so small for such a great reduction in surface deflection. The significance of this is, then, that the optimum Wiener result can be approached closely even with the operation confined to a realistic linear range.

Characteristics of the optimum transfer functions.- It is of interest to consider in greater detail the transfer functions corresponding to the desired operating point in figure 6. This operating point corresponds very closely to a value of $\rho = 10^4$ (see fig. 5) which will therefore be used as an example. In Appendix A the transfer functions of the compensating network, closed-loop system, and open-loop system have been derived. The results are given below; the numerical values of the parameters are summarized in table II.

$$H_{co} = \frac{T_\alpha^2 s^2+2\zeta_\alpha T_\alpha s+1}{(T_\beta s+1)(T_\gamma^2 s^2+2\zeta_\gamma T_\gamma s+1)} \quad \frac{1}{T_u^2 s^2+2\zeta_u T_u s+1} \quad T_\delta^2 \frac{s^2(T_a^2 s^2+2\zeta_a T_a s+1)}{T_v^2 s^2+2\zeta_v T_v s+1} \tag{14}$$

$$Y_o = \frac{T_\alpha^2 s^2+2\zeta_\alpha T_\alpha s+1}{(T_\beta s+1)(T_\gamma^2 s^2+2\zeta_\gamma T_\gamma s+1)} \quad \frac{1}{T_u^2 s^2+2\zeta_u T_u s+1} \quad \frac{T_b^2 s^2+2\zeta_b T_b s+1}{T_v^2 s^2+2\zeta_v T_v s+1} \tag{15}$$

$$\mu_o = k_\mu \underbrace{\frac{T_\alpha^2 s^2+2\zeta_\alpha T_\alpha s+1}{s^2(T_\lambda s+1)}}_{\text{Due to Wiener theory}} \quad \underbrace{\frac{1}{T_x^2 s^2+2\zeta_x T_x s+1}}_{\text{Due to control restriction}} \quad \underbrace{\frac{T_b^2 s^2+2\zeta_b T_b s+1}{T_y^2 s^2+2\zeta_y T_y s+1}}_{\text{Due to aerodynamics}} \tag{16}$$

It is illuminating to trace to their origin the various factors comprising these optimum transfer functions. Analysis shows that terms due to the basic Wiener theory also appear in the modified theory. In addition, other terms due to the aerodynamics and the control-deflection restriction also appear in the solution. This situation is illustrated by the grouping of terms in equations (14), (15), and (16). It can be said that the terms which arise from basic Wiener theory correspond in form to the first group of terms. However, certain constants are somewhat altered, as can be seen from table II by a comparison of the parameters given for the two theories for identical target motion and noise characteristics. The second group of terms in the equations indicates that the optimum form of the filtering term due to control-motion restriction is quadratic.[2] The last group of terms in the transfer functions can be traced to the aerodynamics. In fact, the numerators are identical with terms in the aerodynamic transfer function.

The transfer functions are illustrated in figures 7(a), 7(b), and 7(c); these curves represent the optimum transfer functions in the presence of the control-motion restriction. For comparison purposes the corresponding transfer functions obtained from the Wiener theory are also plotted on these figures. It can be seen that, in general, the transfer functions for these two cases are similar at the very low frequencies and separate to a greater extent as the frequency is increased. The difference is primarily due to filtering terms which are required to satisfy the restriction on control motion.

The added complexity has certain effects on the control motion and error. These effects can best be illustrated by means of the corresponding power spectra, that is, by the integrands in equations (11) and (13). These spectra have been plotted in figures 8 and 9, and for comparison the corresponding curves for the Wiener theory are shown. It can be seen from figure 8 that the spectrum of the control deflection for the more complex system attenuates far more rapidly than does that for the Wiener theory. It is as a result of this fact that the modified system does not limit. As for the error, it is seen from figure 9 that over the important frequency range the error due to noise is not altered too seriously so that most of the increase in the total error is due to an increase in the target motion component.

Effect of noise magnitude on performance.- The preceding results were determined on the basis of a design noise magnitude which lay between the expected extremes. The noise magnitude may vary because of targets of different size, aspect, and turning rate. For this reason the error performance for the optimum transfer function has been determined and is

[2]It is interesting to note that from calculations not presented here it has been observed that the damping ratios of these quadratics always lie between 0.7 and 0.8 over the entire range of control motion presented in figure 6.

shown in figure 10 (curve A) as a function of the zero frequency noise magnitude, N. The error performance shown is optimum only at the design value of noise. Shown for comparison is curve B, which represents the error performance derived from the Wiener theory, corresponding to the same design condition (see ref. 3). The difference between these two curves, then, is the increase in the error as a result of the rms restriction on the control deflection.

As a further comparison two additional curves obtained from reference 3 are shown. First, curve C illustrates the performance of a system (with certain saturable elements) which was optimized for the fastest possible response to a step input in the absence of noise. The performance can be seen to be significantly poorer than the optimum performance given as curve A. Second, the best result that could be obtained in reference 3 is shown as curve D in the figure. The system corresponding to this curve was not optimum because the linear Wiener theory used in this approach was not capable of evaluating all of the various filtering terms discussed in preceding paragraphs. For example, terms due to Wiener theory were not altered, and terms due to aerodynamics were not used. Terms due to control restriction were included but the performance was limited by the arbitrarily assumed form. Thus the system was not optimum and limiting occurred; the performance deteriorated accordingly.

System synthesis.- To achieve the results which have been presented it is necessary to design the guidance system shown in figure 4 to have the optimum transfer function Y_o. This can be done in many different ways since the actual beam-rider system consists of two distinct parts: the tracking radar and the missile-control system. For example, the optimum transfer function Y_o might be split up and apportioned between these two parts of the guidance system. Or, on the other hand, the missile-control system alone might be designed to approximate the optimum Y_o in which case the tracking radar should be designed to have a relatively fast response. In a similar manner the tracking radar could be optimized, in which case the fast response should be designed into the missile-control system.

To investigate all these possibilities is beyond the intended scope of this report. As an example, however, of one possible design the choice of missile-control-system filtering was investigated. For this case it is desired to design the missile-control system to match the optimum transfer function Y_o. This procedure is not unique; the analysis used herein is based primarily on cut-and-try procedures. It has been found that the desired system could be synthesized in a conventional fashion illustrated in figure 11. To show how this system is capable of supplying the optimum filtering the open-loop transfer function has been derived in Appendix B where it is shown that with certain assumptions

$$\mu = \frac{y_M}{\xi} = \frac{k_2 k_s V}{T_d + k_s k_3} \quad \frac{(T_{10}s + 1)(T_4 s + 1)(T_b^2 s^2 + 2\zeta_b T_b s + 1)}{s^2(T_{11}s + 1)(T_5 s + 1)(as^3 + bs^2 + cs + 1)} \tag{17}$$

Comparison with the optimum μ_o in equation (16) shows that certain differences in form exist. However, equation (16) can be expressed in another form by factoring approximately certain quadratic terms which have large damping ratios. Equation (16) can be written then as

$$\mu_o \approx k_\mu \frac{(T_\alpha s + 1)(T_\alpha s + 1)(T_b^2 s^2 + 2\zeta_b T_b s + 1)}{s^2(T_\lambda s + 1)(T_x s + 1)[(T_x s + 1)(T_y^2 s^2 + 2\zeta_y T_y s + 1)]} \tag{18}$$

It is now possible to choose the parameters in equation (17) to match those of equation (18); the specific values are given in table III.

The remainder of the system consists of the tracking radar whose response should be made relatively fast for this design approach. Further, from the plots presented in figures 8 and 9 it is apparent that the tracking radar should be designed so as not to alter appreciably the spectral distribution of error or control motions. Thus a break point or natural frequency of several cycles per second would be satisfactory.

Comparisons and other considerations.- In a REAC simulation of this system its operation was examined in further detail. Of particular importance in this examination was the control deflection and the associated servo energy. It was found that the control deflections were effectively restrained to within the linear range and as a result the servo energy was greatly reduced. For a given servo the power expended is proportional to the time average of the sum of the absolute displacements of control motion. Thus the average servo power over a sufficient time interval of duration t can be determined from

$$\text{average servo power} \sim \frac{\Sigma|\Delta\delta|}{t}$$

For this system there is more than a two-thirds reduction in required servo energy over that for the system with smallest servo energy requirement discussed in reference 3. The saving in servo energy becomes even greater when compared to systems for which the error performance becomes progressively worse than the optimum. The control-deflection time history obtained from the REAC was used to show that the required control rates are easily attainable since they rarely exceeded 3 to 3.5 radians/sec. This system has other virtues. For example, there is also a reduction of voltages within the circuit to reasonable and easily obtainable values.

From this simulation work, then, two facts are apparent. First, it is clear that the validity of applying only a control-motion restriction in the analysis has been verified, since the control rate and system voltages did not saturate. Second, it is apparent that in comparison with systems of reference 3 in which limiting occurred, the present system not only produced a smaller error but was accompanied by other desirable effects such as decreased servo energy and circuit voltage requirements.

The missile-control system discussed in the above paragraphs is intended only as an example designed to achieve optimum performance against noise. It is clear that since the system operation is essentially linear, all designs which approximate the desired Y_o would give approximately the same performance. However, it is often necessary to satisfy other requirements which are related to the specific design objectives of the system and which may favor certain designs or system configurations. Because of the freedom in choice in distributing the optimum filtering in the system, the optimum characteristics specified by the theory do not, in general, place an inherent limitation on satisfying other requirements. For example, requirements on transient response during the beam entry phase may dictate a design in which more of the optimum filtering is located in the tracking radar. Similarly, requirements of simplicity on certain parts of the system may dictate yet a different design. Because these and similar requirements are related to the detailed design objectives, an investigation of such factors is beyond the scope of this report.

CONCLUDING REMARKS

This study has considered the application of Newton's modification of the Wiener filter theory to the choice of optimum transfer function for the beam-rider guidance system. The analysis has been applied to a typical variable-incidence missile at a given flight condition attacking a maneuvering target in the presence of glint noise. By minimizing the mean-square error with a side restriction on the mean-square value of certain quantities, limiting effects, of primary importance in missile guidance, are largely eliminated.

Although many limiting-type nonlinearities are of importance, this study has shown that the critical nonlinearity is due to control-deflection limiting, since a restriction applied to the deflection sufficient to confine control motions to within the linear range also satisfactorily prevented other types of limiting. Results have been given which illustrate the effect of the control-motion restriction on the minimum rms error. Zero restriction corresponds to the Wiener theory whose results are unattainable since impossibly large control motions are demanded. However, as the surface deflection is reduced by means of an increasing restriction, the minimum error increases slowly until at a realistic

value of the control deflection the error has increased only a few feet. Thus it is clear that the optimum performance predicted by the Wiener theory can still be approached closely by confining operation of the system to a realistic linear range.

The transfer functions of the optimum guidance system have been given and have been compared to the corresponding transfer functions from the Wiener theory. Differences were shown to be the result of added filtering terms demanded by the restriction on control motion. The various filtering factors can be traced to their origin. It was shown that terms due to basic Wiener theory appear in the solution, and that the additional terms can be associated with the control-motion restriction and the missile aerodynamics.

For the optimum system, performance against variable noise magnitude was given and was compared to Wiener theory. As an example of one possible design which achieves these results, a missile-control system was synthesized to match the optimum transfer function. In a REAC simulation the operation of this sytem was examined in further detail. It was found that the magnitude of circuit voltages, and control-motion rates are greatly reduced in comparison with systems in which limiting occurs. Similarly, the required servo energies are appreciably reduced, resulting in about a two-thirds saving.

Ames Aeronautical Laboratory
National Advisory Committee for Aeronautics
Moffett Field, Calif., May 11, 1955

APPENDIX A

DETERMINATION OF THE OPTIMUM MODIFIED WIENER FILTER

The solution for the optimum compensating network H_{co} illustrated in figure 3 is given by equation (6) in the text as follows:

$$\left.\begin{aligned} H_{co}(i\omega) &= \frac{1}{2\pi\Lambda^{+}(\omega)} \int_{0}^{\infty} e^{-i\omega t} \int_{-\infty}^{\infty} \frac{\overline{H_f(i\alpha)}\Phi_T(\alpha)e^{i\alpha t}}{\Lambda^{-}(\alpha)} \, d\alpha \, dt \\ \text{where} \quad \Lambda(\omega) &= \left[\overline{H_f(i\omega)}H_f(i\omega) + \rho\right]\Phi_{ii}(\omega) \end{aligned}\right\} \quad (A1)$$

In this equation Φ_{ii} is defined as

$$\Phi_{ii} = \Phi_T + \Phi_N \quad (A2)$$

where Φ_T and Φ_N represent the spectral density of the target motion and noise, respectively. The quantities Λ^{+} and Λ^{-} are defined as the factors of Λ with poles and zeros in the upper and lower half-planes, respectively. Thus

$$\Lambda = \Lambda^{+}\Lambda^{-} \quad (A3)$$

For the case to be considered here the target motion and noise will be taken as

$$\Phi_T = \frac{ka^2}{\pi\omega^4(\omega^2 + k^2)} \quad (A4)$$

$$\Phi_N = N \quad (A5)$$

It will be noted that the noise spectrum has been approximated here by a constant in order to reduce the complexity of the calculations. As shown in reference 3, this approximation is valid because the noise defined by equation (1) is essentially flat compared to the passband of the optimum system. It should also be pointed out that use of equation (A4) leads to certain mathematical difficulties which occur in the process of evaluating the right-hand side of equation (A1), because the theory requires that the poles of Φ_T not be located on the real axis. To avoid these difficulties

it is necessary to modify the target-motion spectral density to the following

$$\Phi_T = \frac{ka^2}{\pi(\omega^2 + \eta_1^2)(\omega^2 + \eta_2^2)(\omega^2 + k^2)} \tag{A6}$$

where η_1 and η_2 are any small real numbers. The solution to equation (A1) will then be a function of $i\omega$, η_1, and η_2. The desired answer is obtained by taking $\lim Y_O(i\omega,\eta_1,\eta_2)$ as η_1 and $\eta_2 \to 0$. However, it can be shown (see ref. 3) that the same answer can be obtained more simply by taking η_1 and η_2 equal to zero as would be obtained from the rigorous process described above.

Now by combining equations (A2), (A4), and (A5),

$$\Phi_{ii}(\alpha) = \Phi_T(\alpha) + \Phi_N(\alpha)$$

$$= N \frac{\alpha^6 + k^2\alpha^4 + (ka^2/\pi N)}{\alpha^4(\alpha^2 + k^2)}$$

$$= N \frac{(\alpha - \alpha_{p1})(\alpha - \alpha_{p2})(\alpha - \alpha_{p3})(\alpha + \alpha_{p1})(\alpha + \alpha_{p2})(\alpha + \alpha_{p3})}{\alpha^4(\alpha + ik)(\alpha - ik)}$$

$$\equiv N \frac{[p(\alpha)][-p(-\alpha)]}{\alpha^4(\alpha + ik)(\alpha - ik)} \tag{A7}$$

where the α_{pm} represent roots in the upper half-plane. The polynomial $p(\alpha)$ is

$$p(\alpha) = \prod_{m=1}^{3} (\alpha - \alpha_{pm})$$

$$\equiv \alpha^3 + b_2\alpha^2 + b_1\alpha + b_O \tag{A8}$$

where

$$\left.\begin{aligned} b_2 &= -(\alpha_{p1} + \alpha_{p2} + \alpha_{p3}) \\ b_1 &= \alpha_{p1}\alpha_{p2} + \alpha_{p1}\alpha_{p3} + \alpha_{p2}\alpha_{p3} \\ b_O &= -\alpha_{p1}\alpha_{p2}\alpha_{p3} \end{aligned}\right\} \tag{A9}$$

In a similar manner

$$-p(-\alpha) = \alpha^3 - b_2\alpha^2 + b_1\alpha - b_0 \tag{A10}$$

An expression to be used later can be obtained from these preceding equations as follows

$$\alpha^6 + k^2\alpha^4 + \frac{ka^2}{\pi N} = (\alpha^3 + b_2\alpha^2 + b_1\alpha + b_0)(\alpha^3 - b_2\alpha^2 + b_1\alpha - b_0)$$

from which

$$-b_0^2 = \frac{ka^2}{\pi N} \tag{A11}$$

The quantity H_f in equation (A1) represents the fixed network or aerodynamics and its general form (ref. 7) is given by

$$H_f(i\alpha) = \frac{y_M}{\delta} = -\frac{1}{T_s^2}\,\frac{[(1 - T_b^2\alpha^2) + i(2\zeta_b T_b\alpha)]}{\alpha^2[(1 - T_a^2\alpha^2) + i(2\zeta_a T_a\alpha)]} \tag{A12}$$

and

$$\overline{H_f(i\alpha)} = -\frac{1}{T_s^2}\,\frac{[(1 - T_b^2\alpha^2) - i(2\zeta_b T_b\alpha)]}{\alpha^2[(1 - T_a^2\alpha^2) - i(2\zeta_a T_a\alpha)]} \tag{A13}$$

Thus

$$\overline{H_f(i\alpha)}H_f(i\alpha) = \frac{1}{T_s^4}\,\frac{[T_b^4\alpha^4 + (4\zeta_b^2T_b^2 - 2T_b^2)\alpha^2 + 1]}{\alpha^4[T_a^4\alpha^4 + (4\zeta_a^2T_a^2 - 2T_a^2)\alpha^2 + 1]} \tag{A14}$$

Accordingly it can be shown that in equation (A1)

$$\overline{H_f(i\alpha)}H_f(i\alpha) + \rho$$

$$= \frac{\rho T_s^4T_a^4\alpha^8+\rho T_s^4(4\zeta_a^2T_a^2-2T_a^2)\alpha^6+(T_b^4+\rho T_s^4)\alpha^4+(4\zeta_b^2T_b^2-2T_b^2)\alpha^2+1}{T_s^4\omega^4[T_a^4\alpha^4+(4\zeta_a^2T_a^2-2T_a^2)\alpha^2+1]}$$

$$= \rho T_a^4\,\frac{\prod_{n=1}^{4}(\alpha-\alpha_{qn})\prod_{n=1}^{4}(\alpha+\alpha_{qn})}{\alpha^4[T_a^4\alpha^4+(4\zeta_a^2T_a^2-2T_a^2)\alpha^2+1]}$$

$$\equiv \rho T_a^4\,\frac{q(\alpha)q(-\alpha)}{\alpha^4[T_a^4\alpha^4+(4\zeta_a^2T_a^2-2T_a^2)\alpha^2+1]} \tag{A15}$$

where the α_{qn} represent roots in the upper half-plane. The polynomial $q(\alpha)$ above is

$$q(\alpha) = \prod_{n=1}^{4} (\alpha - \alpha_{qn})$$

$$\equiv \alpha^4 + c_3\alpha^3 + c_2\alpha^2 + c_1\alpha + c_0 \tag{A16}$$

where

$$\left.\begin{aligned} c_3 &= -(\alpha_{q1} + \alpha_{q2} + \alpha_{q3} + \alpha_{q4}) \\ c_2 &= \alpha_{q1}\alpha_{q2} + \alpha_{q1}\alpha_{q3} + \alpha_{q1}\alpha_{q4} + \alpha_{q2}\alpha_{q3} + \alpha_{q2}\alpha_{q4} + \alpha_{q3}\alpha_{q4} \\ c_1 &= -(\alpha_{q1}\alpha_{q2}\alpha_{q3} + \alpha_{q1}\alpha_{q2}\alpha_{q4} + \alpha_{q1}\alpha_{q3}\alpha_{q4} + \alpha_{q2}\alpha_{q3}\alpha_{q4}) \\ c_0 &= \alpha_{q1}\alpha_{q2}\alpha_{q3}\alpha_{q4} \end{aligned}\right\} \tag{A17}$$

In a similar manner,

$$q(-\alpha) = \alpha^4 - c_3\alpha^3 + c_2\alpha^2 - c_1\alpha + c_0 \tag{A18}$$

An expression to be used later can be obtained from these preceding equations as follows

$$\rho T_s^4 T_a^4 \alpha^8 + \rho T_s^4 (4\zeta_a^2 T_a^2 - 2T_a^2)\alpha^6 + (T_b^4 + \rho T_s^4)\alpha^4 + (4\zeta_b^2 T_b^2 - 2T_b^2)\alpha^2 + 1$$

$$= \rho T_s^4 T_a^4 q(\alpha) q(-\alpha)$$

$$= \rho T_s^4 T_a^4 (\alpha^4 + c_3\alpha^3 + c_2\alpha^2 + c_1\alpha + c_0)(\alpha^4 - c_3\alpha^3 + c_2\alpha^2 - c_1\alpha + c_0)$$

from which

$$c_0^2 = \frac{1}{\rho T_s^4 T_a^4} \tag{A19}$$

The second equation in (A1) can now be found by combining equations (A7) and (A15)

$$\Lambda(\alpha) = \rho T_a^4 N \frac{q(\alpha)q(-\alpha)p(\alpha)[-p(-\alpha)]}{\alpha^8[T_a^4\alpha^4 + (4\zeta_a^2 T_a^2 - 2T_a^2)\alpha^2 + 1](\alpha + ik)(\alpha - ik)} \tag{A20}$$

This expression can be split into two factors with poles and zeros in the upper and lower half-planes. From the preceding definitions $q(\alpha)$ and $p(\alpha)$ both have their zeros in the upper half-plane. Thus

$$\Lambda^{+}(\alpha) = \rho T_a^4 N \frac{q(\alpha)p(\alpha)}{\alpha^4(1 - T_a^2\alpha^2 + i2\zeta_a T_a\alpha)(\alpha - ik)} \tag{A21}$$

$$\Lambda^{-}(\alpha) = \frac{q(-\alpha)[-p(-\alpha)]}{\alpha^4(1 - T_a^2\alpha^2 - i2\zeta_a T_a\alpha)(\alpha + ik)} \tag{A22}$$

Now, let us consider the evaluation of the first integral in equation (A1). This integral can be evaluated by combining equations (A4), (A13), and (A22) as follows:

$$I_1 \equiv \int_{-\infty}^{\infty} \frac{\overline{H_f(\alpha)}\Phi_T(\alpha)e^{i\alpha t}}{\Lambda^{-}(\alpha)}\, d\alpha$$

$$= -\frac{ka^2}{T_s^2\pi} \int_{-\infty}^{\infty} \frac{(1 - T_b^2\alpha^2 - i2\zeta_b T_b\alpha)e^{i\alpha t}}{\alpha^2(\alpha - ik)q(-\alpha)[-p(-\alpha)]}\, d\alpha$$

$$= -\frac{ka^2}{T_s^2\pi} \int_{-\infty}^{\infty} \frac{(1 - T_b^2\alpha^2 - i2\zeta_b T_b\alpha)e^{i\alpha t}}{\alpha^2(\alpha - ik)\prod_{n=1}^{4}(\alpha + \alpha_{qn})\prod_{m=1}^{3}(\alpha + \alpha_{pm})}\, d\alpha$$

$$\equiv -\frac{ka^2}{T_s^2\pi} \int_{-\infty}^{\infty} f(\alpha)d\alpha \tag{A23}$$

where $f(\alpha)$ is defined as the integrand. By considering α to be a complex variable, the integral can be evaluated by a contour integration indicated by the following sketch:

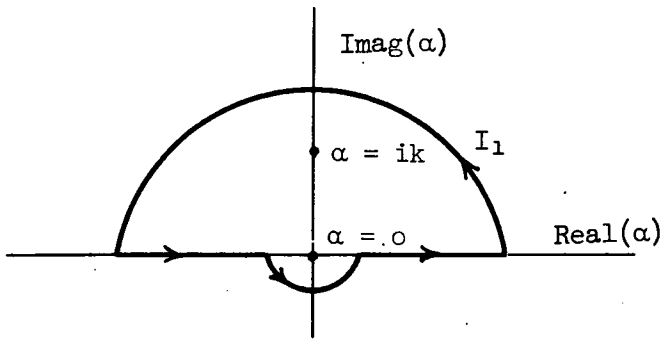

There are two poles within this contour, a second-order pole at the origin and a simple pole at $\alpha = ik$, as indicated. The residues are

$$\text{Res}(o) = \lim_{\alpha \to o} \frac{d}{d\alpha} [\alpha^2 f(\alpha)]$$

$$= \frac{t}{kb_o c_o} - \frac{kb_o c_o 2\zeta_b T_b + ik(b_o c_1 + b_1 c_o) + b_o c_o}{k^2 b_o^2 c_o^2}$$

$$\equiv \frac{t}{kb_o c_o} + \gamma_1 \tag{A24}$$

$$\text{Res}(ik) = \lim_{\alpha \to ik} (\alpha - ik) f(\alpha)$$

$$= \frac{(T_b^2 k^2 + 2\zeta_b T_b k + 1) e^{-kt}}{-k^2 q(-ik)[-p(-ik)]}$$

$$\equiv \gamma_2 e^{-kt} \tag{A25}$$

Now, by means of the residue theory, the value of the integral is given by

$$I_1 = - \frac{2ika^2}{T_s^2} [\text{Res}(o) + \text{Res}(ik)]$$

Thus from equations (A24) and (A25),

$$I_1 = - \frac{2ika^2}{T_s^2} \left(\gamma_1 + \frac{t}{kb_o c_o} + \gamma_2 e^{-kt} \right) \tag{A26}$$

The second integral in equation (A1) is denoted by I_2 and is merely the Fourier transform of I_1. Hence

$$I_2 = \int_o^\infty I_1 e^{-i\omega t} dt$$

$$= - \frac{2ika^2}{T_s^2} \int_o^\infty \left[\gamma_1 e^{-i\omega t} + \frac{t}{kb_o c_o} e^{-i\omega t} + \gamma_2 e^{-(k+i\omega)t} \right] dt \tag{A27}$$

Thus it can be shown that

$$I_2 = -\frac{2ika^2}{T_s^2 b_o c_o}\frac{(\gamma_1+\gamma_2)b_o c_o(i\omega)^2 + [k\gamma_1 b_o c_o + (1/k)]i\omega + 1}{(i\omega)^2(k+i\omega)}$$

$$\equiv -\frac{2ika^2}{T_s^2 b_o c_o}\frac{T_\alpha^2(i\omega)^2 + 2\zeta_\alpha T_\alpha(i\omega) + 1}{(i\omega)^2(k+i\omega)} \qquad (A28)$$

It should be noted that since the η's were assumed to be zero, questions concerning the existence of the above integral arise. However, as indicated in reference 3, when the analysis is made without this assumption, the integral in equation (A27) does exist, and the limit of this integral as the η's approach zero becomes precisely equation (A28).

The coefficients can be expressed in a more convenient form by eliminating the intermediate parameters γ_1 and γ_2 by means of definitions given in equations (A24) and (A25). The following results are then obtained:

$$2\zeta_\alpha T_\alpha = k\gamma_1 b_o c_o + \frac{1}{k}$$

$$= -2\zeta_b T_b - i\frac{b_o c_1 + b_1 c_o}{b_o c_o} \qquad (A29)$$

Also

$$T_\alpha^2 = (\gamma_1+\gamma_2)b_o c_o$$

$$= -\frac{b_o c_o(T_b^2 k^2 + 2\zeta_b T_b K + 1)}{k^2 q(-ik)[-p(-ik)]} - \frac{kb_o c_o 2\zeta_b T_b + ik(b_o c_1 + b_1 c_o)}{k^2 b_o c_o} - \frac{1}{k^2} \qquad (A30)$$

For the missile parameters of table I and the value of k given on page 28

$$T_b^2 k^2 + 2\zeta_b T_b k + 1 \approx 1$$

so that very nearly

$$T_\alpha^2 = -\frac{b_o c_o}{k^2 q(-ik)[-p(-ik)]} + \frac{2\zeta_\alpha T_\alpha}{k} - \frac{1}{k^2} \qquad (A31)$$

Now, from equation (A1) the optimum compensating network can be determined as follows:

$$H_{co}(i\omega) = \frac{I_2}{2\pi\Lambda^+(\omega)} \tag{A32}$$

Substituting equations (A21) and (A28) into (A32) gives

$$H_{co}(i\omega) = -\frac{ka^2}{\pi N\rho T_s^2 T_a^4 b_o c_o} \frac{(i\omega)^2[T_\alpha^2(i\omega)^2+2\zeta_\alpha T_\alpha(i\omega)+1][T_a^2(i\omega)^2+2\zeta_a T_a(i\omega)+1]}{p(\omega)q(\omega)} \tag{A33}$$

To reduce this expression to a more standard form it can be seen from equation (A16) that

$$q(\omega) = \prod_{n=1}^{4} (\omega - \alpha_{qn}) = c_o \prod_{n=1}^{4} \left(-\frac{\omega}{\alpha_{qn}} + 1\right) \tag{A34}$$

Similarly from equation (A8)

$$p(\omega) = \prod_{m=1}^{3} (\omega - \alpha_{pm}) = b_o \prod_{m=1}^{3} \left(-\frac{\omega}{\alpha_{pm}} + 1\right) \tag{A35}$$

Also by using the definitions given in equations (A11) and (A19) the compensating network can be shown to reduce to

$$H_{co}(i\omega) = T_s^2 \frac{(i\omega)^2[T_\alpha^2(i\omega)^2 + 2\zeta_\alpha T_\alpha(i\omega) + 1][T_a^2(i\omega)^2 + 2\zeta_a T_a(i\omega) + 1]}{\prod_{m=1}^{3}\left(-\frac{\omega}{\alpha_{pm}} + 1\right)\prod_{n=1}^{4}\left(-\frac{\omega}{\alpha_{qn}} + 1\right)} \tag{A36}$$

By the substitution of the conventional complex frequency s for $i\omega$

$$H_{co}(s) = T_s^2 \frac{s^2(T_\alpha^2 s^2 + 2\zeta_\alpha T_\alpha s + 1)(T_a^2 s^2 + 2\zeta_a T_a s + 1)}{\prod_{m=1}^{3}\left(\frac{is}{\alpha_{pm}} + 1\right)\prod_{n=1}^{4}\left(\frac{is}{\alpha_{qn}} + 1\right)} \tag{A37}$$

It is shown later in the numerical examples that certain terms combine to give quadratic factors as shown below

$$H_{co}(s) = T_s^2 \frac{s^2(T_\alpha^2 s^2+2\zeta_\alpha T_\alpha s+1)(T_a^2 s^2+2\zeta_a T_a s+1)}{(T_\beta s+1)(T_\gamma^2 s^2+2\zeta_\gamma T_\gamma s+1)(T_u^2 s^2+2\zeta_u T_u s+1)(T_v^2 s^2+2\zeta_v T_v s+1)} \tag{A38}$$

where

$$T_\beta = \frac{i}{\alpha_{p1}} \qquad T_u^2 = -\frac{1}{\alpha_{q1}\alpha_{q2}}$$

$$T_\gamma^2 = -\frac{1}{\alpha_{p2}\alpha_{p3}} \qquad 2\zeta_u T_u = i\frac{\alpha_{q1}+\alpha_{q2}}{\alpha_{q1}\alpha_{q2}}$$

$$2\zeta_\gamma T_\gamma = i\frac{\alpha_{p2}+\alpha_{p3}}{\alpha_{p2}\alpha_{p3}} \qquad T_v^2 = -\frac{1}{\alpha_{q3}\alpha_{q4}}$$

$$2\zeta_v T_v = i\frac{\alpha_{q3}+\alpha_{q4}}{\alpha_{q3}\alpha_{q4}}$$

The compensating network given in equation (A38) can be used to determine the over-all transfer function Y_o. From figure 2

$$Y_o(s) = H_{co}(s)H_f(s) \tag{A39}$$

Substitution of equations (A12) and (A38) into (A39) gives

$$Y_o(s) = \frac{(T_\alpha^2 s^2+2\zeta_\alpha T_\alpha s+1)(T_b^2 s^2+2\zeta_b T_b s+1)}{(T_\beta s+1)(T_\gamma^2 s^2+2\zeta_\gamma T_\gamma s+1)(T_u^2 s^2+2\zeta_u T_u s+1)(T_v^2 s^2+2\zeta_v T_v s+1)} \tag{A40}$$

If Y_o is considered to represent a unity feedback system, the equivalent open-loop transfer function is shown in the later specific example to be of the following form:

$$\mu_o(s) = \frac{Y_o(s)}{1 - Y_o(s)}$$

$$= k_\mu \frac{(T_\alpha^2 s^2 + 2\zeta_\alpha T_\alpha s + 1)(T_b^2 s^2 + 2\zeta_b T_b s + 1)}{s^2(T_\lambda s + 1)(T_x^2 s^2 + 2\zeta_x T_x s+1)(T_y^2 s^2 + 2\zeta_y T_y s + 1)} \tag{A41}$$

Because ζ_α and ζ_x are close enough to unity (table II) it is possible to factor the corresponding terms approximately to give

$$\mu_o(s) \approx k_\mu \frac{(T_\alpha s + 1)(T_\alpha s + 1)(T_b^2 s^2 + 2\zeta_b T_b s + 1)}{s^2(T_\lambda s + 1)(T_x s + 1)[(T_x s + 1)(T_y^2 s^2 + 2\zeta_y T_y s + 1)]} \tag{A42}$$

The numerical evaluation of the optimum system has been carried out for the following values of target motion and noise:

$k = 0.4$ $\qquad$ $a = 1$ g

$\bar{T} = 5$ sec $\qquad$ $N = 15$ ft^2/radian/sec

From this example ρ will be taken to be 10^4 since, as shown in the text, this value results in a near-optimum restriction on control deflection.

Evaluation of the numerator in equation (A7) gives

$$\alpha^6 + k^2\alpha^4 + \frac{ka^2}{\pi N} = \alpha^6 + 0.16\,\alpha^4 + 8.8$$

$$= \prod_{m=1}^{3} (\alpha - \alpha_{pm}) \prod_{m=1}^{3} (\alpha + \alpha_{pm})$$

where

$$\alpha_{p1} = i\,1.456$$

$$\alpha_{p2} = 1.427 \exp(i\,0.543)$$

$$\alpha_{p3} = -1.427 \exp(-i\,0.543)$$

which are all located in the upper half of the complex α plane. Then from equation (A9)

$$b_2 = -i\,2.94$$

$$b_1 = -4.201$$

$$b_0 = i\,2.97$$

Similarly from equation (A15) for $\rho = 10^4$,

$$\rho T_s^4 T_a^4 \alpha^8 + \rho T_s^4 (4\zeta_a^2 T_a^2 - 2T_a^2)\alpha^6 + (T_b^4 + \rho T_s^4)\alpha^4 + (4\zeta_b^2 T_b^2 - 2T_b^2)\alpha^2 + 1$$

$$= (22.58 \times 10^{-8})\alpha^8 - (7.475 \times 10^{-5})\alpha^6 + (6.267 \times 10^{-3})\alpha^4 - (0.006094)\alpha^2 + 1$$

$$= \rho T_s^4 T_a^4 \prod_{n=1}^{4} (\alpha - \alpha_{qn}) \prod_{n=1}^{4} (\alpha + \alpha_{qn})$$

Solving for the roots gives

$$\alpha_{q1} = 3.593 \exp(0.804)$$

$$\alpha_{q2} = -3.593 \exp(-0.804)$$

$$\alpha_{q3} = 12.92 \exp(0.804)$$

$$\alpha_{q4} = -12.92 \exp(-0.804)$$

which again are all in the upper-half α plane. From the definitions in equation (A17),

$$c_3 = -i\ 6.677$$

$$c_2 = -187.61$$

$$c_1 = i\ 883.40$$

$$c_0 = 2155$$

Now from the values of the roots α_{pm} and α_{qn} as well as the b and c coefficients, the optimum compensating network can be calculated by means of equation (A38). For this purpose it is necessary to evaluate the left-hand sides of equations (A29), (A31), and the parameters following equation (A38). Results of these calculations are given in table II in terms of damping ratios and undamped natural periods. Substitution of these parameters in equations (A38) and (A40) gives

$$H_{co}(s) = 7.91\times10^{-4} \frac{s^2(1.28\ s^2+1.82\ s+1)(0.00602\ s^2+0.00830\ s+1)}{(0.687\ s+1)(0.490\ s^2+0.727\ s+1)(0.0775\ s^2+0.401\ s+1)(0.006\ s^2+0.009\ s+1)} \quad (A43)$$

$$Y_o(s) = \frac{(1.28\ s^2+1.82\ s+1)(0.00305\ s^2+0.00243\ s+1)}{(0.687\ s+1)(0.490\ s^2+0.727\ s+1)(0.0775\ s^2+0.401\ s+1)(0.006\ s^2+0.009\ s+1)} \quad (A44)$$

Also included in this table are the parameters of the equivalent open-loop transfer function (eq. (A41)) which is

$$\mu_o(s) = 3.2 \frac{(1.28\ s^2 + 1.82\ s + 1)(0.00305\ s^2 + 0.00243\ s + 1)}{s^2(2.5\ s + 1)(0.0338\ s^2 + 0.266\ s + 1)(0.00619\ s^2 + 0.00807\ s + 1)} \quad (A45)$$

CONFIDENTIAL

APPENDIX B

MISSILE-CONTROL-SYSTEM APPROXIMATION TO THE OPTIMUM TRANSFER FUNCTION

The optimum linear system is illustrated in figure 11. In the following section the system equations are derived.

Using figure 11 it can be shown that

$$\frac{\psi}{E_N} = \frac{k_s(T_M s + 1)(T_3 s + 1)}{T_d s(T_1 s + 1)(T_a^2 s^2 + 2\zeta_a T_a s + 1)(T_3 s + 1) + k_s k_3 s(T_M s + 1)(T_2 s + 1)} \tag{B1}$$

To simplify equation (B1) it is convenient to make $T_3 = T_M$. This assumption is not essential but its use leads to simpler equations. In certain cases where gust disturbances are serious it may be more desirable to choose T_3 small. With the former choice

$$\frac{\psi}{E_N} = \frac{k_s(T_M s+1)}{s[(T_d T_a^2 T_1)s^3+(T_d T_a^2+T_d 2\zeta_a T_a T_1)s^2+(T_d T_1+T_d 2\zeta_a T_a+k_s k_3 T_2)s+(T_d+k_s k_3)]}$$

$$= \frac{k_s}{T_d+k_s k_3} \frac{(T_M s+1)}{s(as^3+bs^2+cs+1)} \tag{B2}$$

where

$$\left.\begin{aligned} a &= \frac{T_d T_a^2 T_1}{T_d + k_s k_3} \\ b &= \frac{T_d(T_a^2 + 2\zeta_a T_a T_1)}{T_d + k_s k_3} \\ c &= \frac{2\zeta_a T_a T_d + T_1 T_d + k_s k_3 T_2}{T_d + k_s k_3} \end{aligned}\right\} \tag{B3}$$

Thus the entire open-loop transfer function can be written as

$$\mu = \frac{y_M}{\xi} = \frac{k_2 k_s V}{T_d + k_s k_3} \frac{(T_{10}s + 1)(T_4 s + 1)(T_b^2 s^2 + 2\zeta_b T_b s + 1)}{s^2(T_{11}s + 1)(T_5 s + 1)(as^3 + bs^2 + cs + 1)} \tag{B4}$$

By comparison with equation (A42) it can be seen to be of the same form as the optimum transfer function. Thus the following correspondences between quantities in equations (B4) and (A42) are appropriate:

$$\left.\begin{aligned} T_{11} &\leftrightarrow T_\lambda \\ T_5 &\leftrightarrow T_x \\ T_{10} &\leftrightarrow T_\alpha \\ T_4 &\leftrightarrow T_\alpha \end{aligned}\right\} \tag{B5}$$

Also it is apparent that

$$\left.\begin{aligned} a &\leftrightarrow T_x T_y^2 \\ b &\leftrightarrow T_y^2 + T_x 2\zeta_y T_y \\ c &\leftrightarrow T_x + 2\zeta_y T_y \end{aligned}\right\} \tag{B6}$$

For these values of a, b, and c, equations (B3) can be solved for the remaining parameters to give

$$\left.\begin{aligned} T_1 &= \frac{aT_a}{bT_a - a2\zeta_a} \\ k_s k_3 &= \frac{T_d T_a^2 T_1 - aT_d}{a} \\ T_2 &= \frac{cT_d + ck_s k_3 - 2\zeta_a T_a T_d - T_1 T_d}{k_s k_3} \end{aligned}\right\} \tag{B7}$$

The value of k_2k_s is determined from the desired gain:

$$k_2k_s \longleftrightarrow k_\mu \frac{T_d + k_sk_3}{V} \tag{B8}$$

Since only k_2k_s and k_sk_3 are specified, one of the three gains k_2, k_3, or k_s may be chosen arbitrarily, subject to the condition that voltage limiting does not occur. From the above equations the system parameters have been determined and are tabulated in table III.

REFERENCES

1. Wiener, Norbert: The Extrapolation, Interpolation, and Smoothing of Stationary Time Series With Engineering Applications. The Technology Press, M.I.T., 1949.

2. Levinson, Norman: A Heuristic Exposition of Wiener's Mathematical Theory of Prediction and Filtering. Appendix C of Extrapolation, Interpolation, and Smoothing of Stationary Time Series with Engineering Applications by Norbert Wiener. The Technology Press, M.I.T., 1949.

3. Stewart, Elwood C.: Application of Statistical Theory to Beam-Rider Guidance in the Presence of Noise. I - Wiener Filter Theory. NACA RM A55E11, 1955.

4. Newton, George C., Jr.: Compensation of Feedback-Control Systems Subject to Saturation. Parts I and II. Jour. Franklin Inst., vol. 254, no. 4, Oct. 1952, pp. 281-296; and no. 5, Nov. 1952, pp. 391-413.

5. Weinstock, Robert: Calculus of Variations With Applications to Physics and Engineering. McGraw-Hill Book Co., Inc., 1952.

6. James, H. M., Nichols, N. B., and Phillips, R. S.: Theory of Servomechanisms. McGraw-Hill Book Co., Inc., 1947.

7. Matthews, Howard F., and Stewart, Elwood C.: A Comparison of the Calculated Maximum-Maneuver Response Characteristics of Three Air-to-Air, Beam-Rider, Guided Missiles Having Different Lift Ratios. NACA RM A51F18, 1951.

8. Hoel, Paul Gerhard: Introduction to Mathematical Statistics. John Wiley and Sons, Inc., 1947, p. 243.

TABLE I.- SUMMARY OF AERODYNAMIC PARAMETERS FOR EXAMPLE MISSILE

Parameter	Value
T_a	0.0775
T_b	.0552
T_d	2.087
T_s^2	.0007911
T_M	.846
ζ_a	.0536
ζ_b	.0220

TABLE II.- SUMMARY OF PARAMETERS OF OPTIMUM TRANSFER FUNCTIONS

Parameter	Modified Wiener theory value	Wiener theory value
T_α	1.13	0.925
ζ_α	.805	.765
T_β	.687	.687
T_γ	.700	.700
ζ_γ	.519	.519
T_λ	2.5	2.5
k_μ	3.2	7.42
T_u	.278	---
ζ_u	.720	---
T_v	.0774	---
ζ_v	.0581	---
T_x	.184	---
ζ_x	.722	---
T_y	.0787	---
ζ_y	.0513	---

TABLE III.- SUMMARY OF PARAMETERS OF OPTIMUM SYSTEM

Parameter	Value
k_2	0.0538
T_4	1.13
T_{10}	1.13
T_{11}	2.5
T_5	.184
k_s	.0463
T_1	.186
k_3	-.674
T_2	.373
T_3	.846

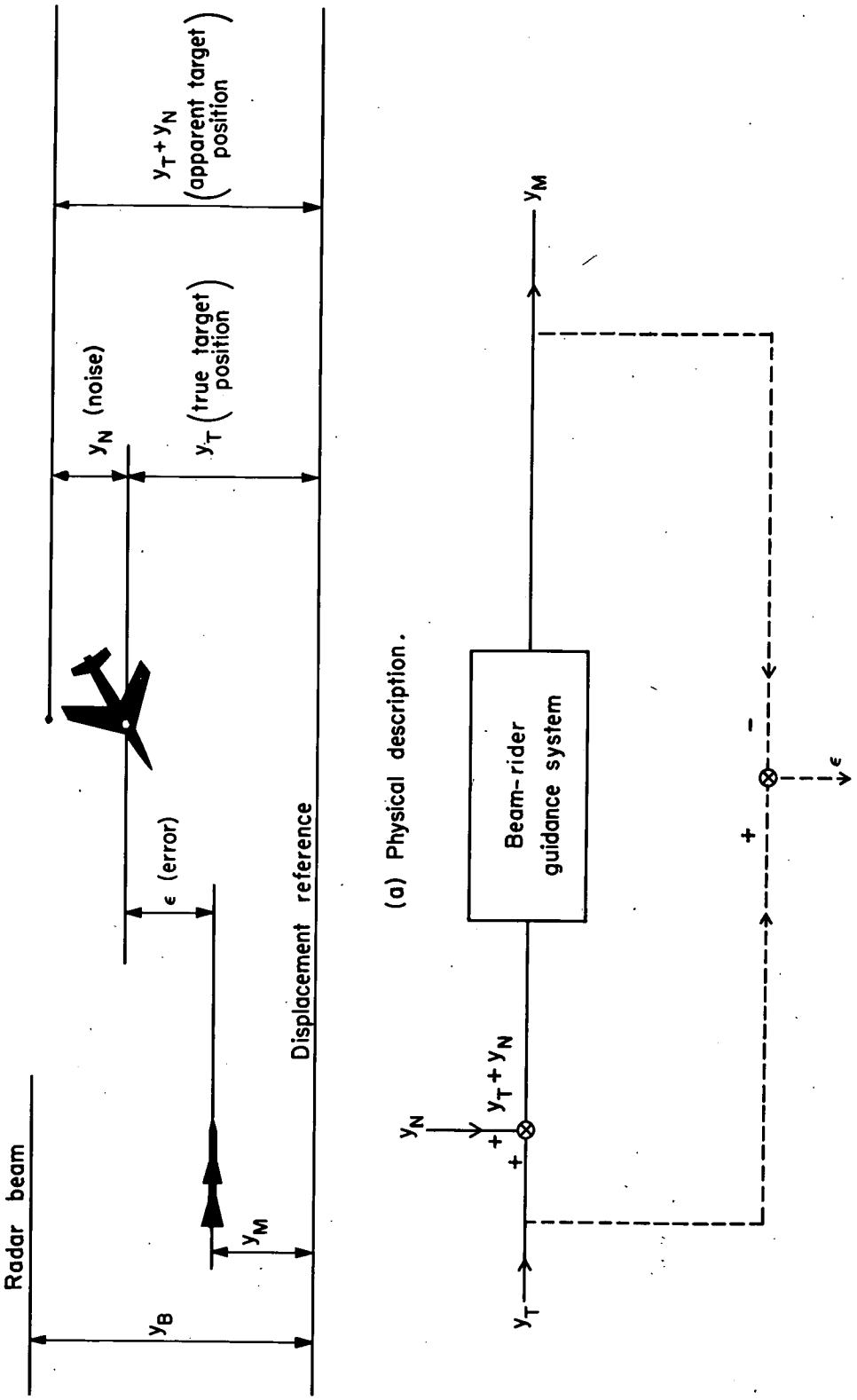

Figure 1.- Beam-rider guidance system.

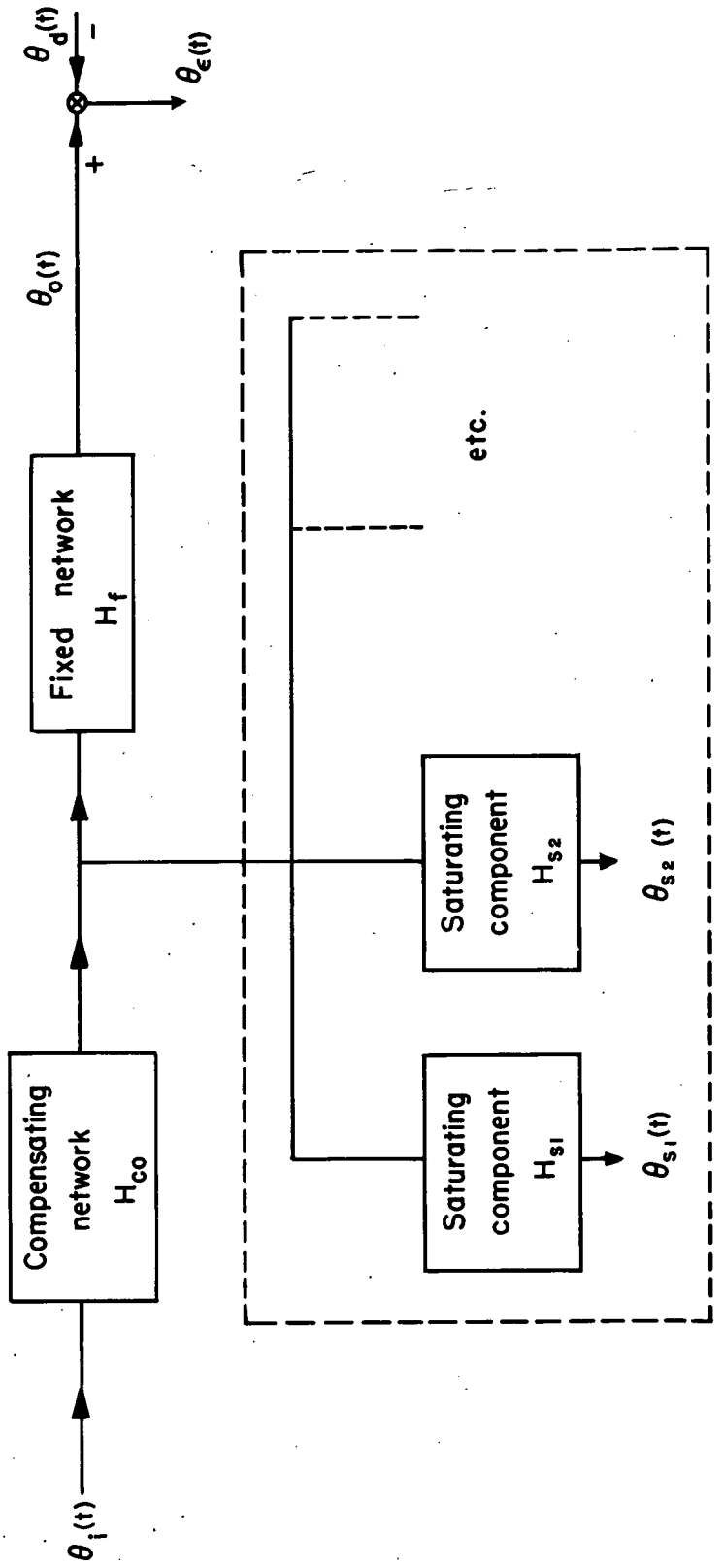

Figure 2.- Block diagram of general filter problem with restrictions.

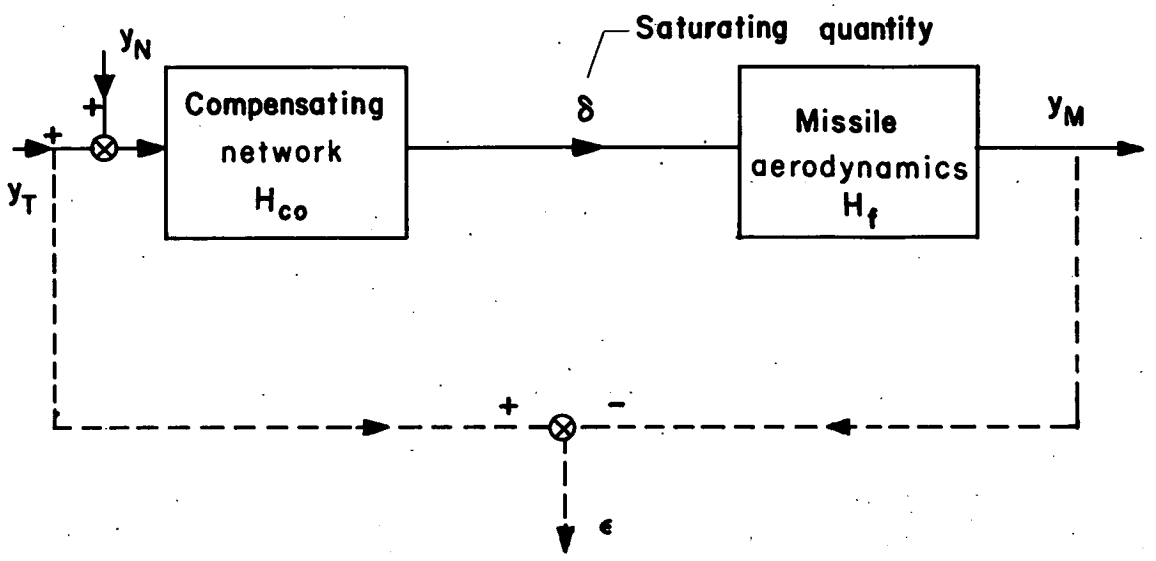

Figure 3.- Block diagram of filter problem for the beam-rider system.

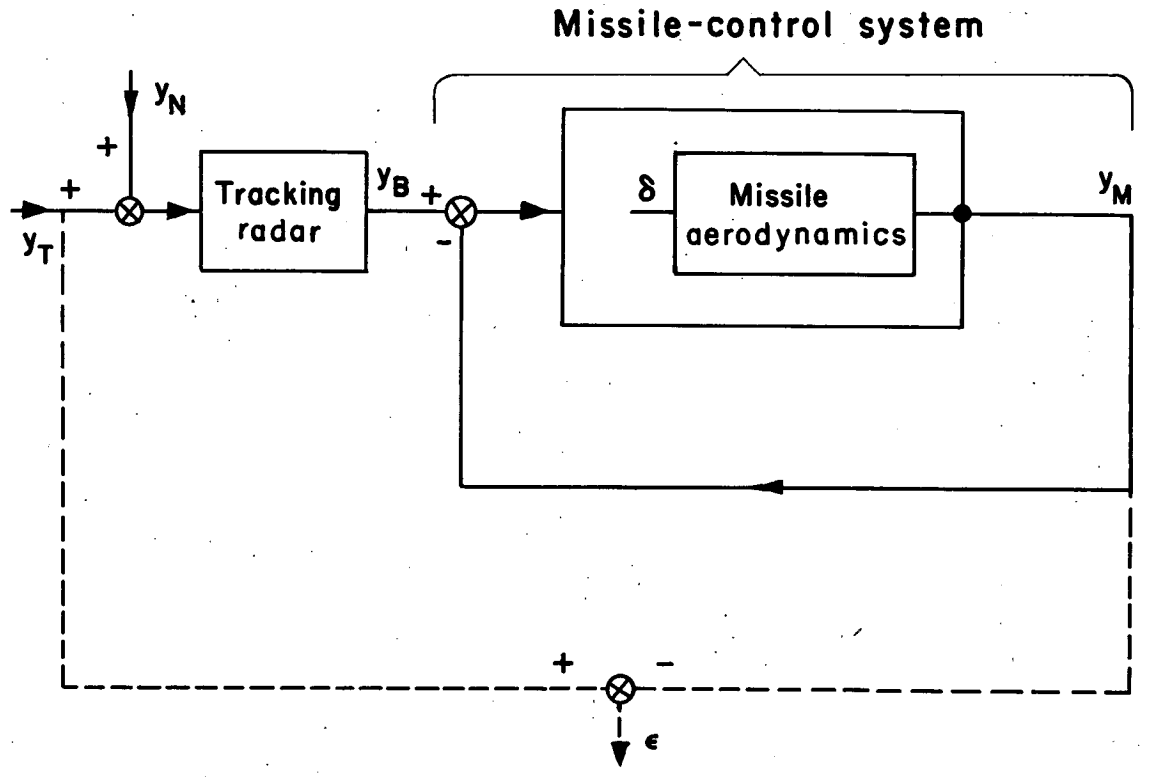

Figure 4.- The beam-rider system.

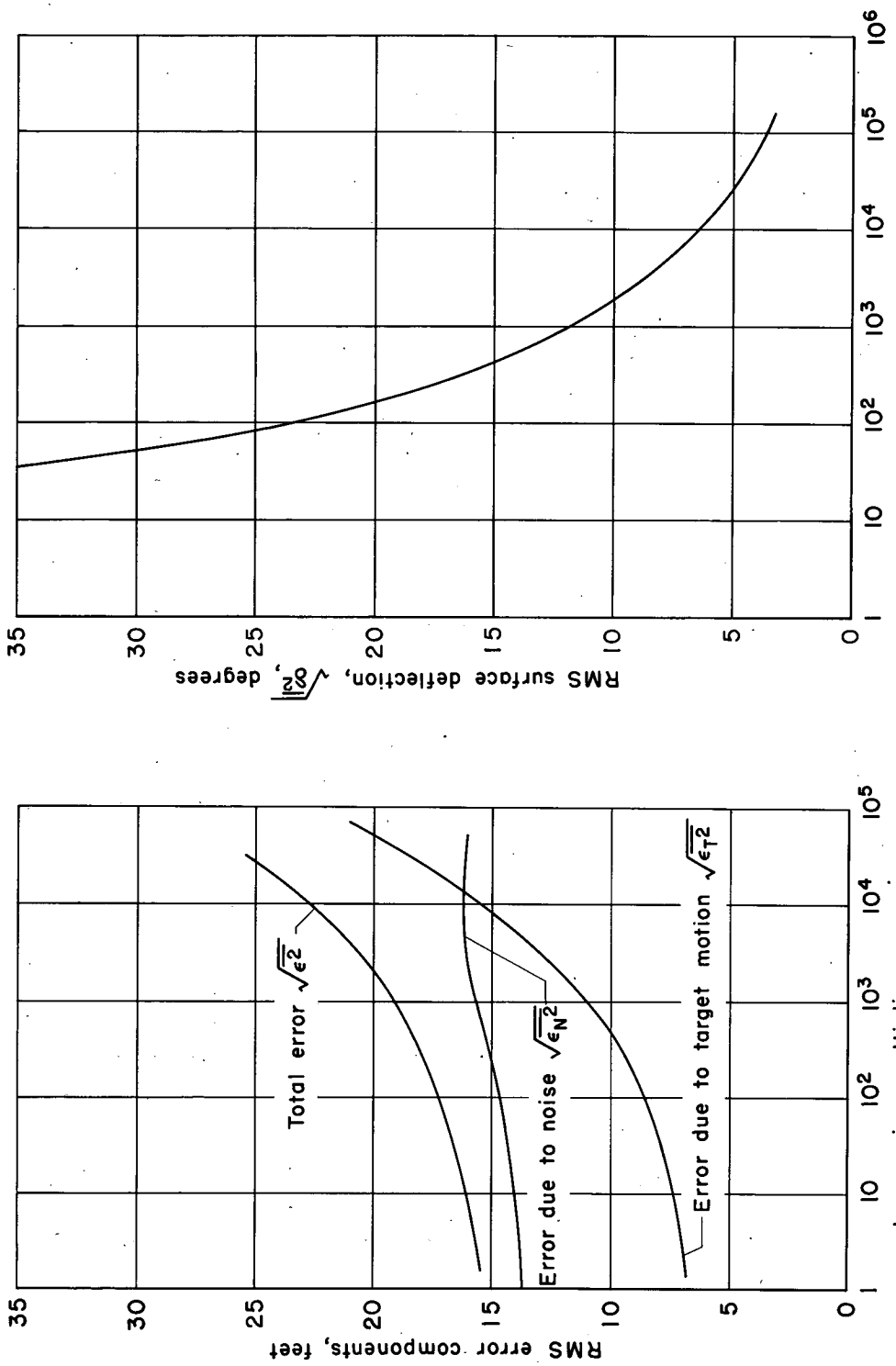

(a) RMS error.

(b) RMS surface deflection.

Figure 5.- Variation of error and control motion with Lagrangian multiplier ρ.

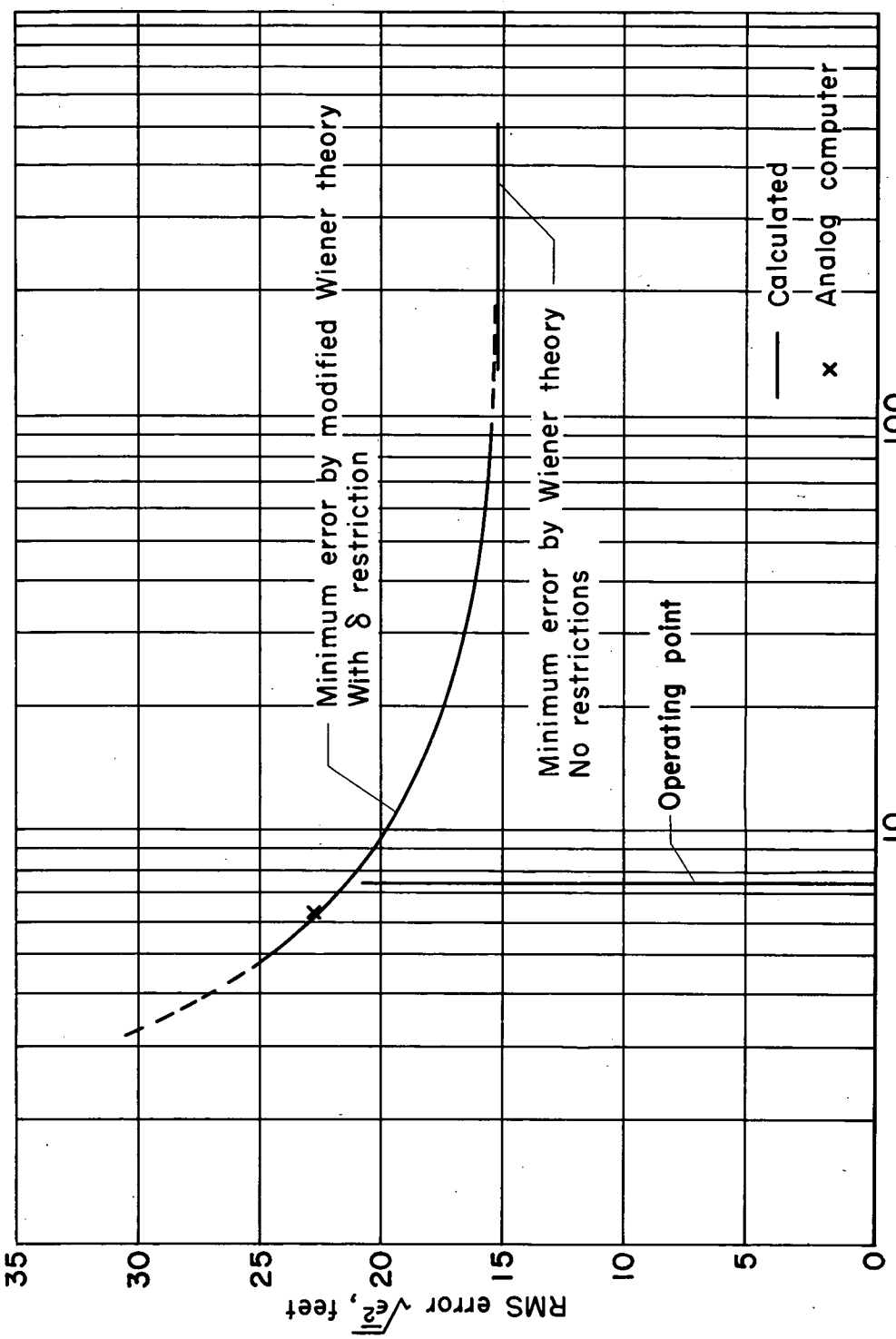

Figure 6.- Effect of rms control motion on minimum rms error.

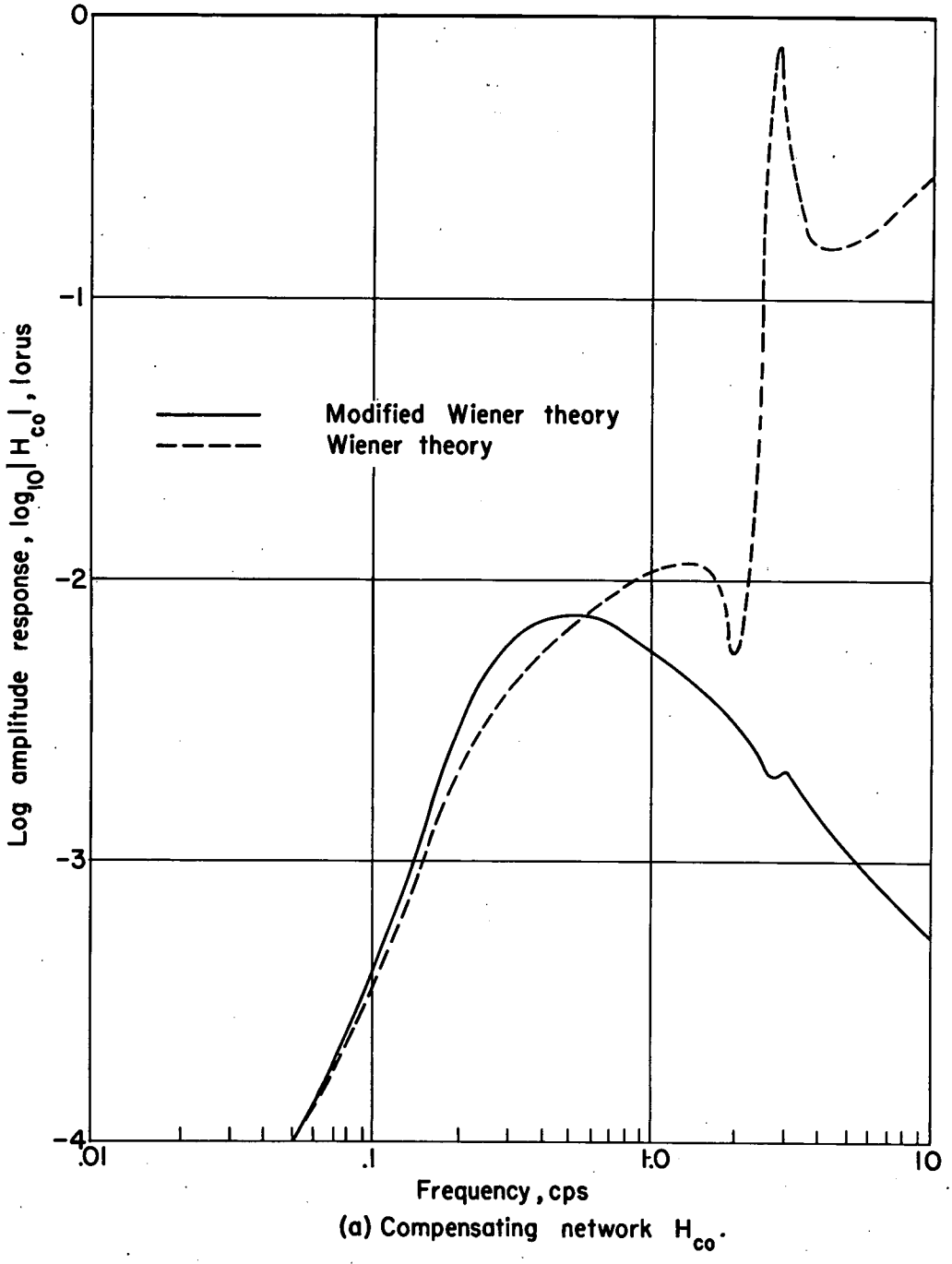

Figure 7.- Optimum transfer functions.

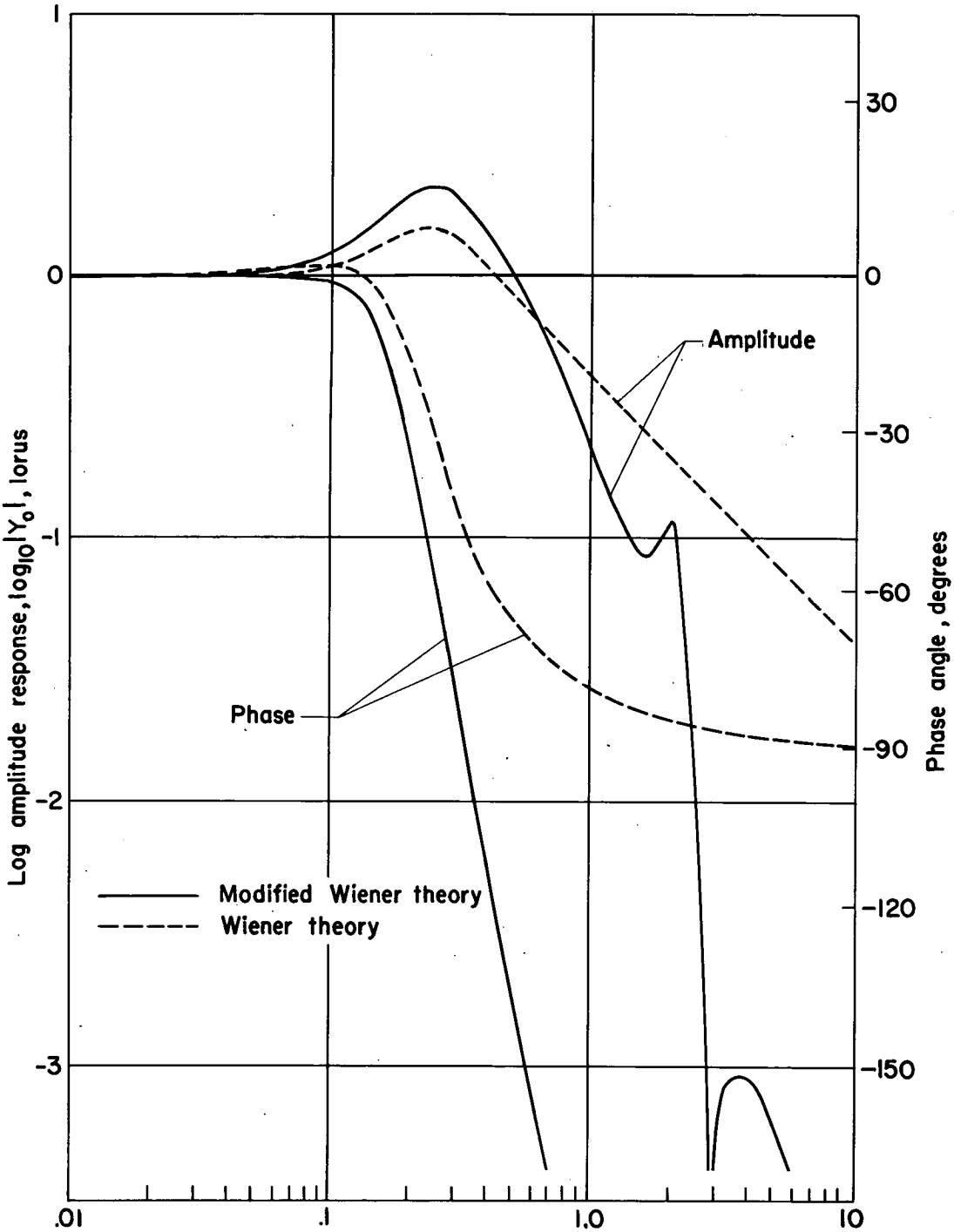

(b) Closed-loop transfer function Y_o.

Figure 7.- Continued.

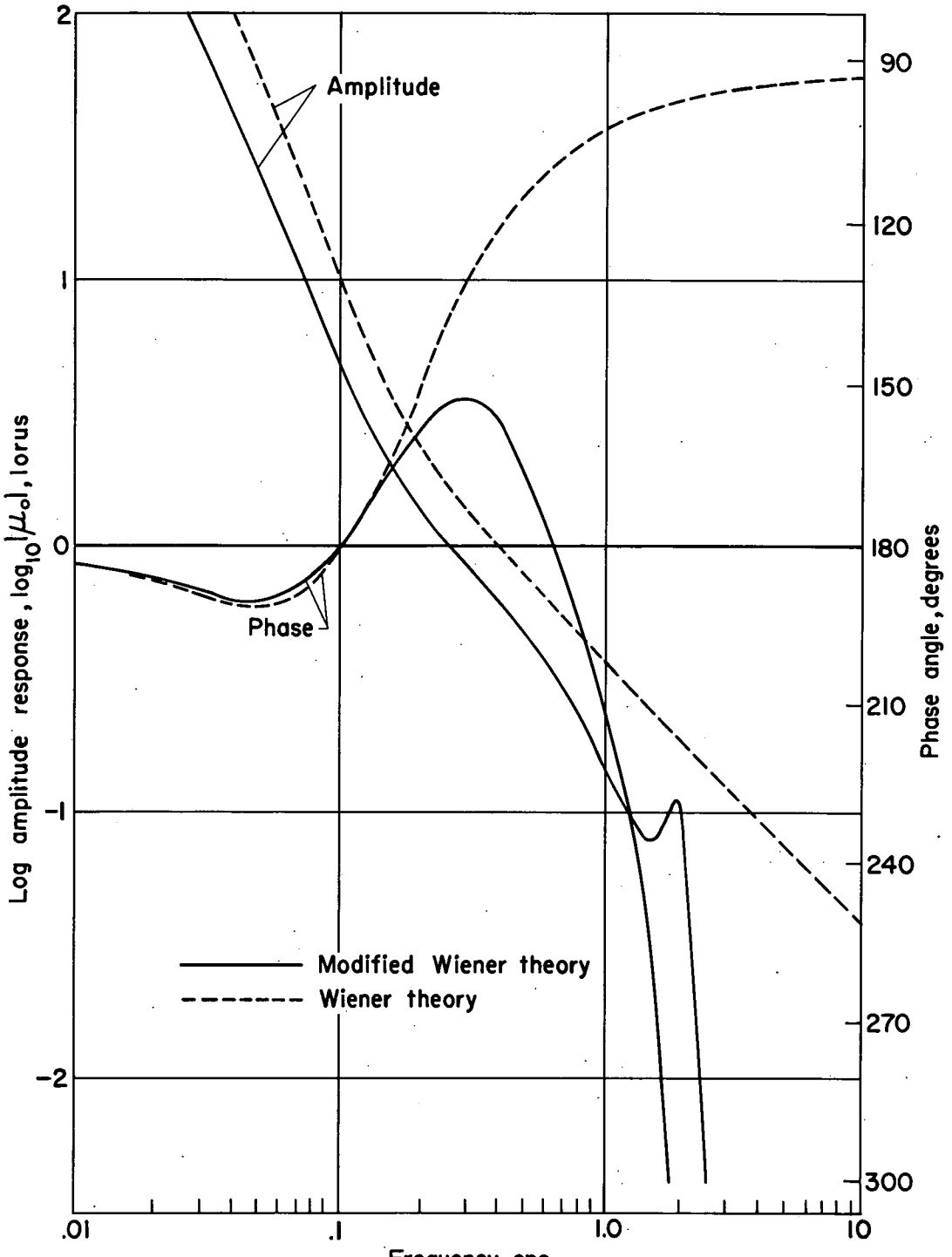

(c) Open-loop transfer function μ_o.

Figure 7.- Concluded.

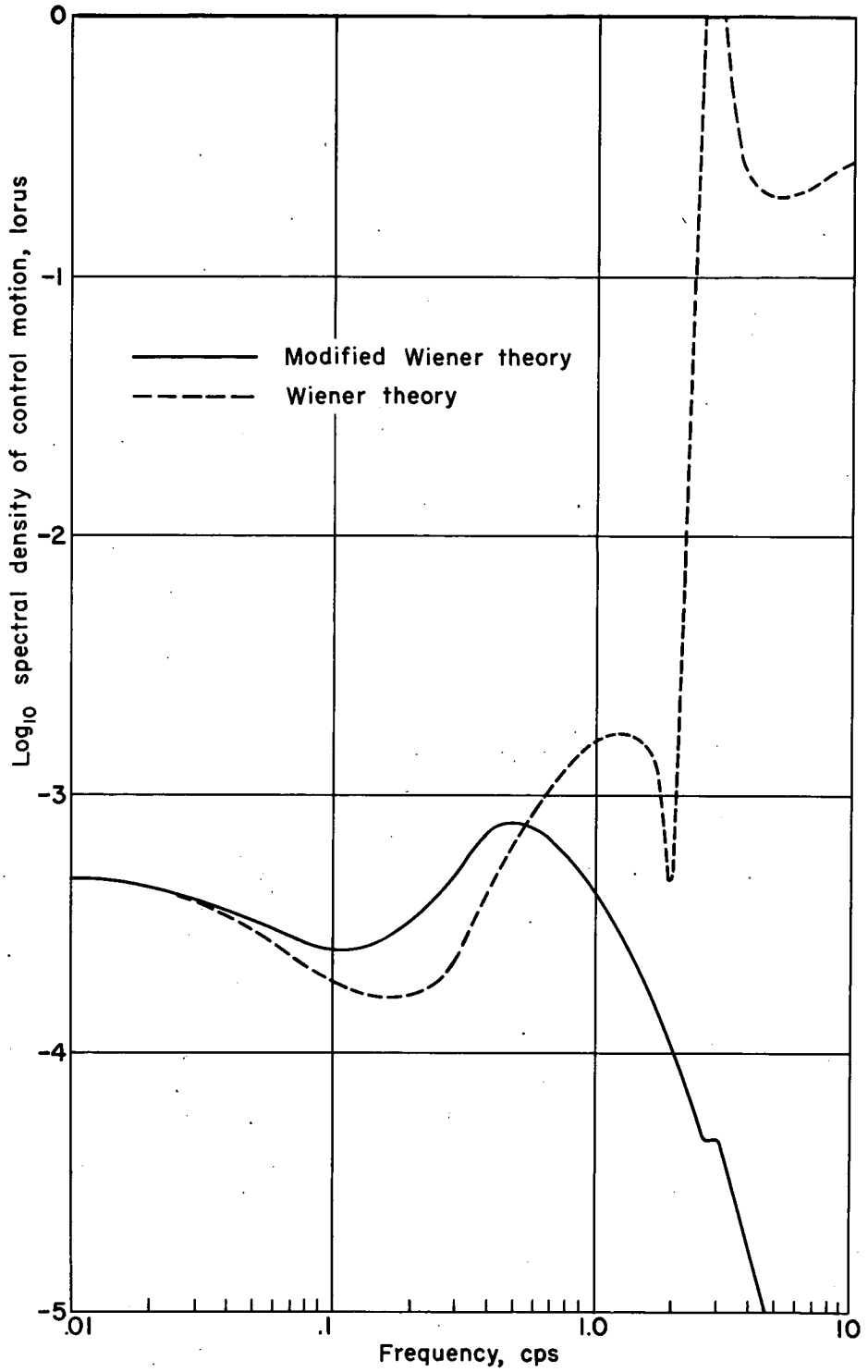

Figure 8.- Spectral density of control motion.

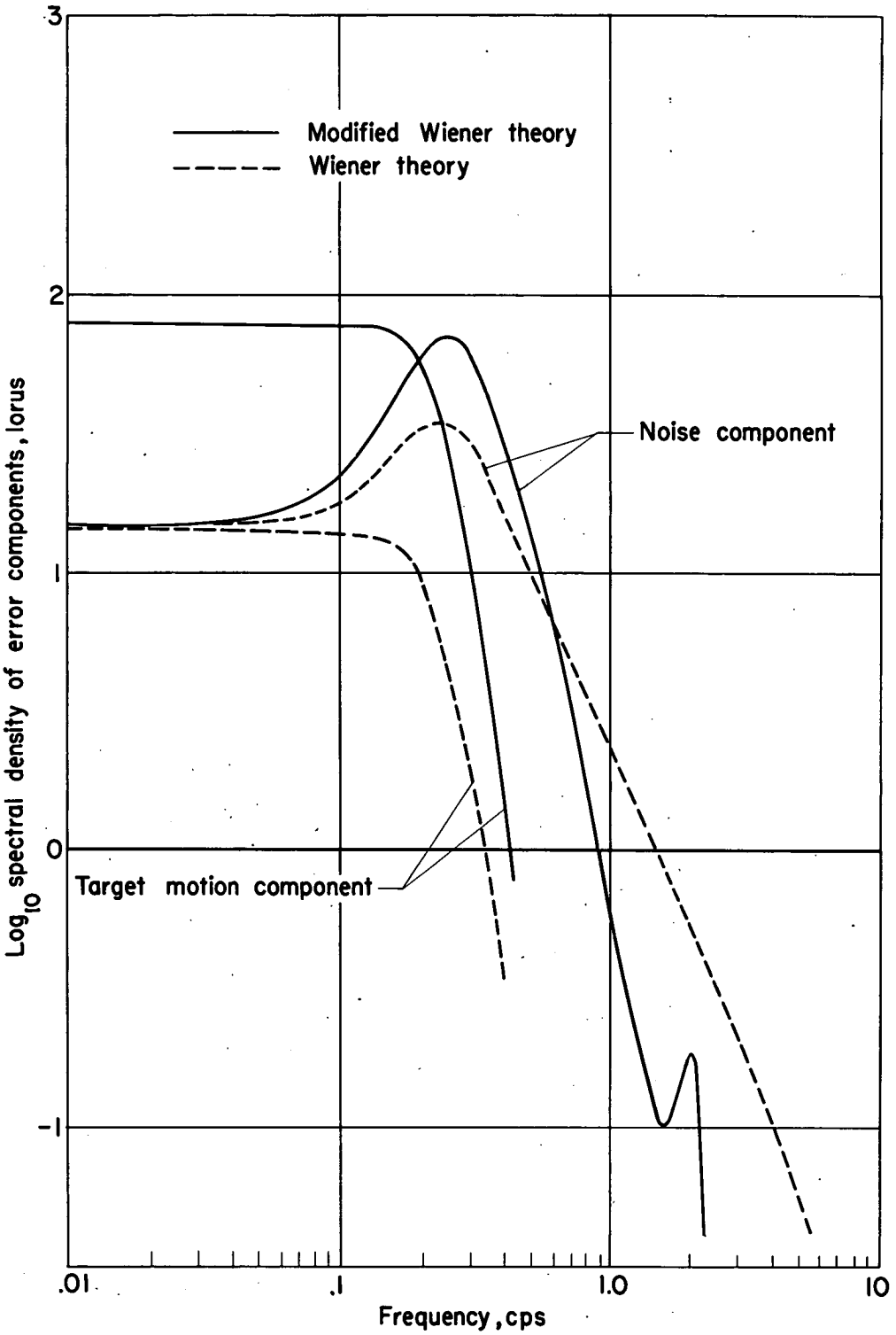

Figure 9.- Spectral density of error components.

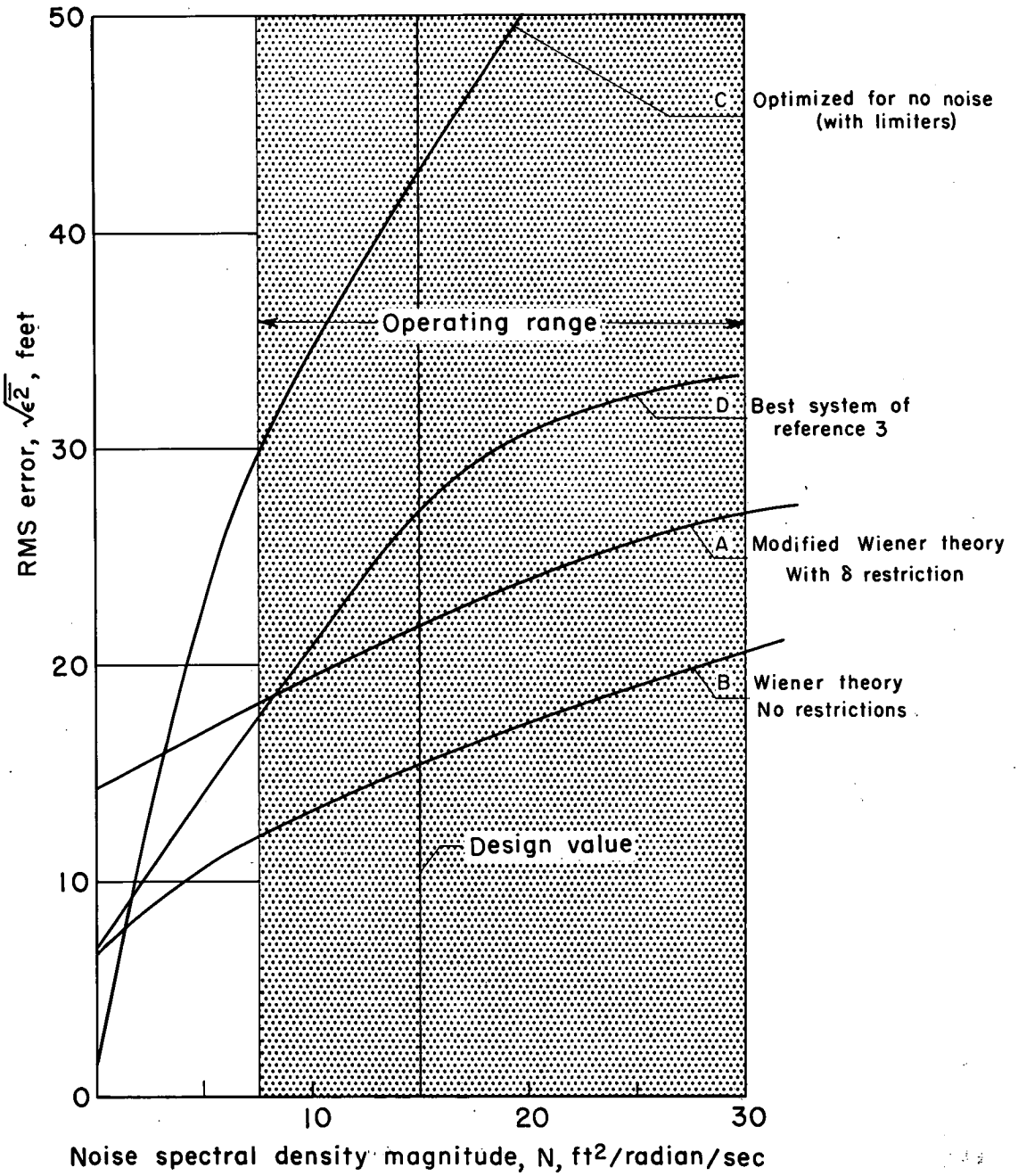

Figure 10.- Comparison of rms error performance of modified Wiener theory with that for various systems; optimized for design value.

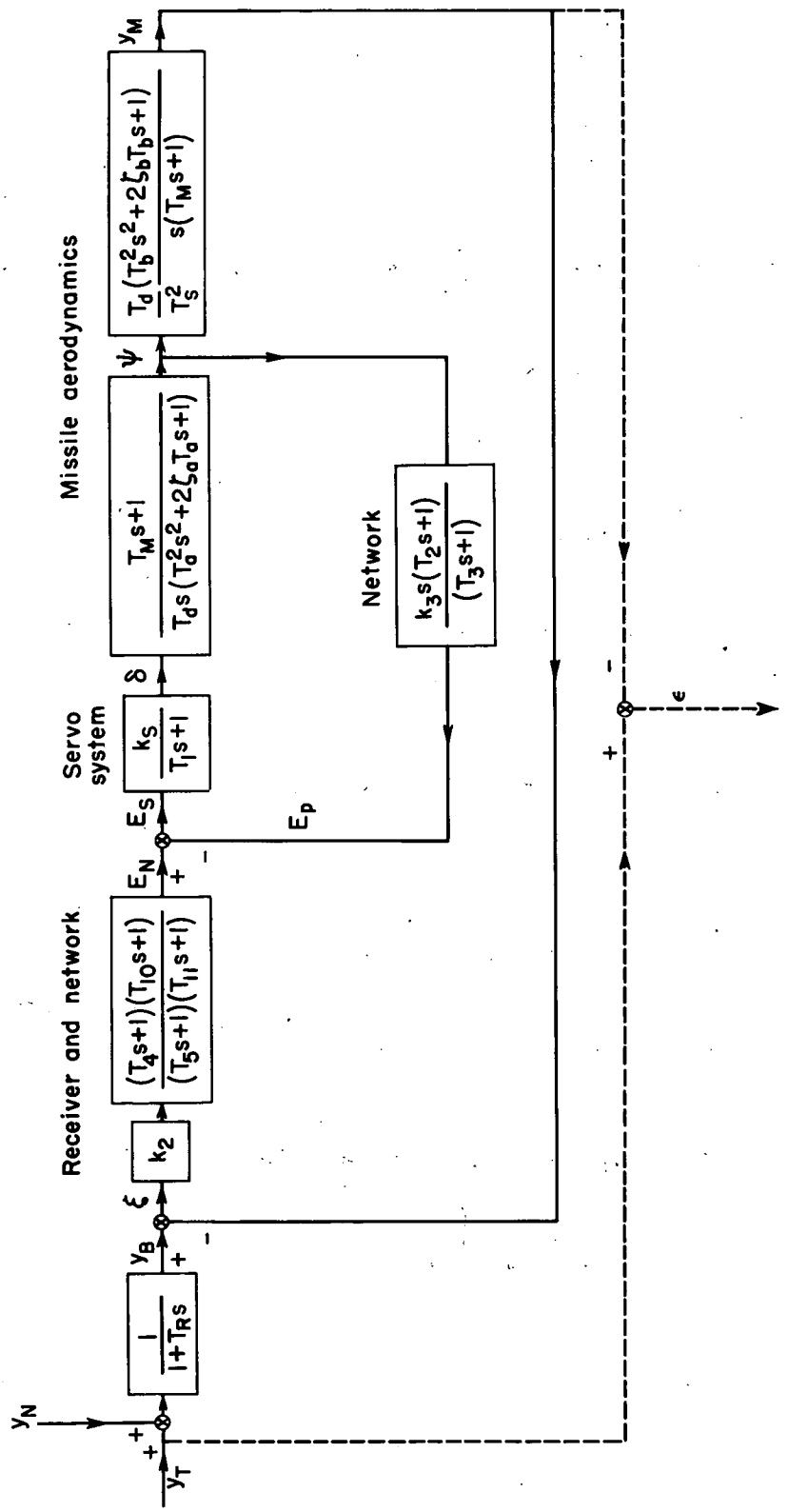

Figure 11.- System approximation of optimum transfer function with control motion restriction.

NACA - Langley Field, Va.